# **Learning Pattern-Specific Experts for Time Series Forecasting Under Patch-level Distribution Shift**

Yanru Sun, Zongxia Xie, Emadeldeen Eldele<sup>‡†</sup>, Dongyue Chen, Qinghua Hu, Min Wu<sup>‡\*</sup>
College of Intelligence and Computing, Tianjin University, China

<sup>‡</sup>I2R, Agency for Science, Technology and Research, Singapore.

<sup>†</sup>Department of Computer Science, Khalifa University, UAE.

{yanrusun, dyuechen, huqinghua}@tju.edu.cn, caddiexie@hotmail.com,

emad0002@ntu.edu.sg, wumin@a-star.edu.sg

#### **Abstract**

Time series forecasting, which aims to predict future values based on historical data, has garnered significant attention due to its broad range of applications. However, real-world time series often exhibit heterogeneous pattern evolution across segments, such as seasonal variations, regime changes, or contextual shifts, making accurate forecasting challenging. Existing approaches, which typically train a single model to capture all these diverse patterns, often struggle with the pattern drifts between patches and may lead to poor generalization. To address these challenges, we propose **TFPS**, a novel architecture that leverages pattern-specific experts for more accurate and adaptable time series forecasting. TFPS employs a dual-domain encoder to capture both time-domain and frequency-domain features, enabling a more comprehensive understanding of temporal dynamics. It then performs subspace clustering to dynamically identify distinct patterns across data segments. Finally, these patterns are modeled by specialized experts, allowing the model to learn multiple predictive functions. Extensive experiments on real-world datasets demonstrate that TFPS outperforms state-of-the-art methods, particularly on datasets exhibiting significant distribution shifts. The data and code are available: https://github.com/syrGitHub/TFPS.

# 1 Introduction

Time series forecasting plays a critical role in various domains, such as finance [18], weather [3, 63, 24], traffic [35, 22], and others [59, 33, 68], by modeling the relationship between historical data and future outcomes. However, the inherent complexity of time series data, including temporal dependencies and non-stationarity, poses significant challenges in achieving reliable forecasts.

Recent Transformer-based models have shown great promise in time series forecasting due to their ability to model long-range dependencies [29, 53]. In particular, models like PatchTST [44] split continuous time series into discrete patches and process them with Transformer blocks. While these models are effective, a closer examination reveals that patches often exhibit distribution shifts, which are frequently associated with concept drift [36]. For example, patches from different regimes, seasons, or operating modes may not only differ in statistical properties [27], but also in the functional relationships between historical and future values [60, 56]. However, this variability contradicts the assumptions of most existing models [44, 69, 9], which adopt the Uniform Distribution Modeling (UDM) strategy by treating all patches as samples from a single underlying distribution. This oversimplified view ignores structural heterogeneity and temporal variation across segments, thereby limiting the model's ability to generalize and degrading its forecasting performance [43, 25].

<sup>\*</sup>Corresponding author

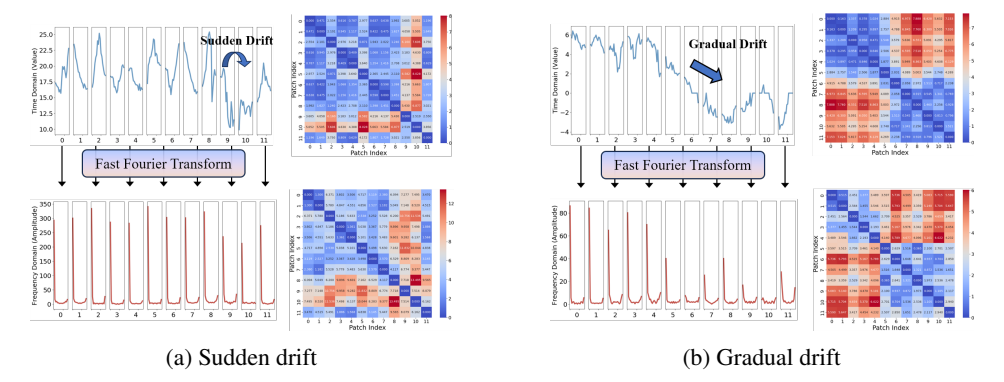


Figure 1: Illustration of distribution shifts between time series patches on the ETTh1 dataset, quantified by Wasserstein distance. The combined time- and frequency-domain views reveal richer and more complementary shift patterns arising from temporal non-stationarity.

To quantify these distributional shifts, we split the ETTh1 dataset into patches and analyze two representative cases: sudden drift and gradual drift, in both time and frequency domains. Specifically, we compute the Wasserstein distance between patches and visualize the results as heatmaps in Figure 1, which clearly illustrate the discrepancies across segments. Notably, sudden drift (Figure 1 (a)) leads to a sharp discrepancy between patches 9 and 10 and the remaining segments, while gradual drift (Figure 1 (b)) reveals that patches 0 to 5 differ from patches 6 to 11, exhibiting a progressive shift that makes forecasting more challenging. Furthermore, the frequency domain offers a complementary perspective on the shifts [42]. These observations highlight the complex and evolving nature of time series data, where different segments may follow distinct distributions and exhibit heterogeneous temporal patterns [55, 27, 17, 56, 52].

To address the challenges posed by distribution shifts in time series data, we propose a novel Time-Frequency Pattern-Specific (TFPS) architecture to effectively model the complex temporal patterns. In particular, TFPS consists of the following three key components. The first is a Dual-Domain Encoder (DDE), which extracts features from both time and frequency domains to provide a comprehensive representation of the time series data, enabling the model to capture both short-term and long-term dependencies. Second, TFPS addresses the issue of concept drift by incorporating a Pattern Identifier (PI), that utilizes a subspace clustering approach to dynamically identify the distinct patterns across patches. This enables the model to effectively handle nonlinear cluster boundaries and accurately assign patches to their corresponding clusters. Finally, TFPS constructs a Mixture of Pattern Experts (MoPE)—a set of specialized expert models, each tailored to a specific pattern identified by the PI. By dynamically assigning patches to the appropriate experts, TFPS learns pattern-specific predictive functions that effectively capture heterogeneous temporal dynamics and distributional variations. This specialized modeling strategy enhances the model's adaptability and yields significant forecasting improvements, particularly on datasets with severe distributional drift.

In summary, the key contributions of this work are:

- We introduce a novel pattern-specific forecasting paradigm that enables segment-wise expert
  modeling based on latent pattern structure, overcoming the limitations of uniform modeling
  under distribution shift.
- We propose TFPS, a dual-domain framework that integrates time- and frequency-domain representations with subspace clustering and dynamic expert routing, enabling the model to explicitly adapt to concept drift and capture evolving patterns in non-stationary time series.
- We evaluate our approach on nine real-world multivariate time series datasets, demonstrating its effectiveness. Our model achieves top-1 performance in 57 out of 72 settings, showcasing its competitive edge in improving forecasting accuracy.

# 2 Related Work

Time Series Forecasting Models. In recent years, deep models with elaborately designed architectures have achieved great progress in time series forecasting [51, 67, 28, 45]. Approaches like TimesNet [61] and ModernTCN [41] utilize convolutional neural networks with time-series-specific modifications, making them better suited for forecasting tasks. Additionally, simpler architectures such as Multi-Layer Perceptron (MLP)-based models [69, 8] have demonstrated competitive performance. However, Transformer-based models have gained particular prominence due to their ability to model long-term dependencies in time series [70, 62, 71, 29]. Notably, PatchTST [44] has become a widely adopted Transformer variant, introducing a channel-independent patching mechanism to enhance temporal representations. This approach has been further extended by subsequent models [29, 9].

While previous work has primarily focused on capturing nonlinear dependencies in time series through enhanced model structures, our approach addresses the distribution shifts caused by evolving patterns within the data, which is a key limitation of existing methods.

**Non-stationary Time Series Forecasting.** Non-stationarity in time series data complicate predictive modeling, necessitating effective solutions to handle shifting distributions [36, 11]. To address varying distributions, normalization techniques have emerged as a focal point in recent research, aiming to mitigate non-stationary elements and align data with a consistent distribution.

For instance, adaptive norm [46] applies z-score normalization using global statistics and DAIN [47] introduces a neural layer for adaptively normalizing each input instance. Reversible instance normalization (RevIN) [20] is proposed to alleviate series shift. Furthermore, Non-stationary transformer [31] points that directly stationarizing time series will damage the model's capability to capture specific temporal dependencies and introduces an innovative de-stationary attention mechanism within self-attention frameworks. Recent advancement include Dish-TS [10], which identifies both intra-and inter-space distribution shifts in time series data, and SAN [34], which applies normalization at the slice level, thus opening new avenues for handling non-stationary time series data. Lastly, SIN [17] introduces a novel method to selecting the statistics and learning normalization transformations to capture local invariance in time series data.

However, normalization methods can only address changes in statistical properties, and over-reliance on them may lead to over-stationarization, where meaningful temporal variations are inadvertently smoothed out [34]. In contrast, our approach preserves the intrinsic non-stationarity of the original series in the latent representation space, enabling the model to better adapt to evolving regimes by tailoring experts to diverse temporal patterns and distributional structures.

# 3 Method

#### 3.1 Preliminaries

Time series forecasting aims to uncover relationships between historical time series data and future data. Let  $\mathcal{X}$  denote the time series, and  $x_t$  represent the value at timestep t. Given the historical time series data  $X = [x_{t-L+1}, \cdots, x_t] \in \mathbb{R}^{L \times C}$ , where L is the length of the look-back window and C > 1 is the number of features in each timestep, the objective is to predict the future series  $Y = [x_{t+1}, \cdots, x_{t+H}] \in \mathbb{R}^{H \times C}$ , where H is the forecast horizon.

#### 3.2 Overall Architecture

Our model introduces three novel components: the Dual-Domain Encoder (DDE), the Pattern Identifier (PI), and the Mixture of Pattern Experts (MoPE), as illustrated in Figure 2. The DDE goes beyond traditional time-domain encoding by incorporating a frequency encoder that applies Fourier analysis, transforming time series data into the frequency domain. This enables the model to capture periodic patterns and frequency-specific features, providing a more comprehensive understanding of the data. The PI is a clustering-based module that distinguishes patches with distinct patterns, effectively addressing the variability in the data. MoPE then utilizes multiple MLP-based experts, each dedicated to modeling a specific pattern, thereby enhancing the model's ability to adapt to the temporal dynamics of time series. Collectively, these components form a cohesive framework that effectively handles concept drift between patches, leading to more accurate time series forecasting.

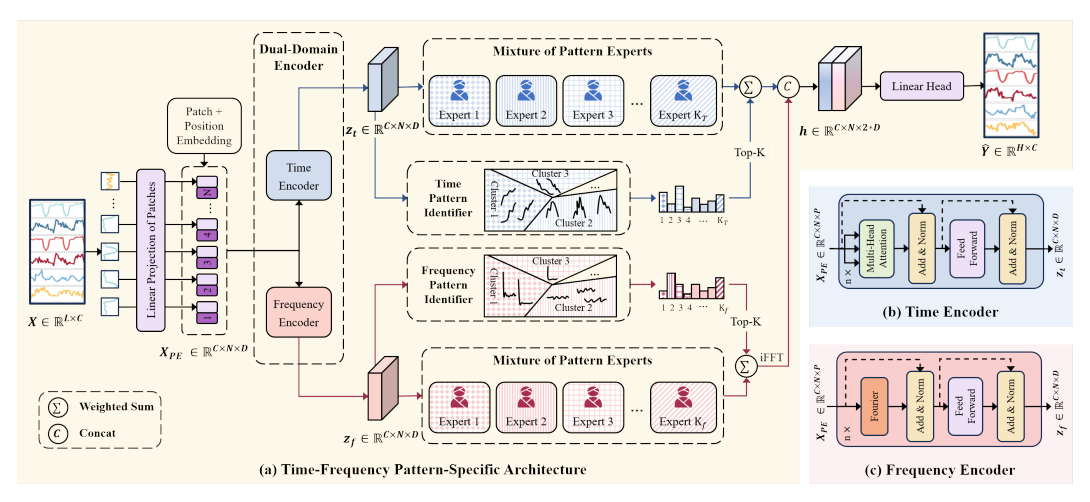


Figure 2: The structure of our proposed TFPS. The input time series is divided into patches, and positional embeddings are added. These embeddings are processed through two branches: time-domain branch and frequency-domain branch. Each branch consists of three key components: (1) an encoder to capture patch-wise features, (2) a clustering mechanism to identify patches with similar patterns, and (3) a mixture of pattern experts block to model the patterns of each cluster. Finally, the outputs from both branches are combined for the final prediction.

#### 3.3 Embedding Layer

Firstly, the input sequence  $X \in \mathbb{R}^{L \times C}$  is divided into patches of length P, resulting in  $N = \lfloor \frac{(L-P)}{S} + 2 \rfloor$  tokens, where S denotes the stride, defining the non-overlapping region between consecutive patches. Each patch is denoted as  $\mathcal{P}_i \in \mathbb{R}^{C \times P}$ . These patches are then projected into a new dimension D, via a linear transformation, such that,  $\mathcal{P}_i \to \mathcal{P}_i' \in \mathbb{R}^{C \times D}$ .

Next, positional embeddings are added to each patch to preserve the temporal ordering disrupted during the segmentation process. The position embedding for the i-th patch, denoted as  $E_i$ , is a vector of the same dimension as the projected patch. The enhanced patch is computed by summing the original patch and its positional embedding:  $X_{PE_i} = \mathcal{P}'_i + E_i$ , and  $X_{PE} = \{X_{PE_1}, X_{PE_2}, \cdots, X_{PE_N}\}$ . Notably, the positional embeddings are learnable parameters, which enables the model to capture the temporal dependencies in the time series more effectively. As a result, the final enriched patch representations are  $X_{PE} \in \mathbb{R}^{C \times N \times D}$ .

## 3.4 Dual-Domain Encoder

As shown in Figure 1, both time and frequency domains reveal distinct concept drifts that can significantly affect the performance of forecasting models. To effectively address these drifts, we propose a Dual-Domain Encoder (DDE) architecture that captures both temporal and frequency dependencies inherent in time series data.

We utilize the patch-based Transformer [44] as an encoder to extract embeddings for each patch, capturing the global trend feature. The multi-head attention is employed to obtain the attention output  $\mathbf{O}_t \in \mathbf{R}^{N \times D}$ :

$$\mathbf{O}_{t} = \operatorname{Attention}(Q, K, V) = \operatorname{Softmax}\left(\frac{QK^{T}}{\sqrt{d_{k}}}\right)V,$$

$$Q = X_{PE}\mathbf{W}_{Q}, \quad K = X_{PE}\mathbf{W}_{K}, \quad V = X_{PE}\mathbf{W}_{V}.$$
(1)

The encoder block also incorporates BatchNorm layers and a feed-forward network with residual connections, as shown in Figure 2 (b). This process generates the temporal features  $z_t \in \mathbb{R}^{C \times N \times D}$ .

In parallel with the time encoder, we incorporate a Frequency Encoder by replacing the self-attention sublayer of the Transformer with a Fourier sublayer [26]. This sublayer applies a 2D Fast Fourier Transform (the number of patches, hidden dimension) to the patch representation, expressed as:

$$\mathbf{O}_f = \mathcal{F}_{patch}(\mathcal{F}_h(X_{PE})). \tag{2}$$

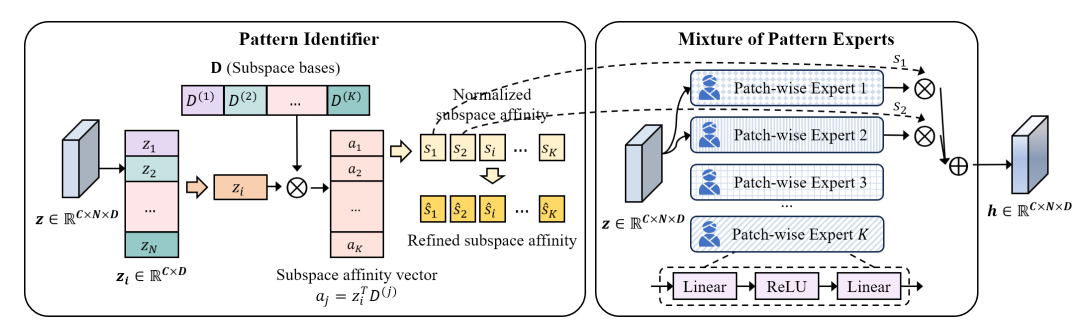


Figure 3: Illustration of the proposed Pattern Identifier and Mixture of Pattern Experts. The embedded representation  $\mathbf{z}$  from DDE combines with subspace  $\mathbf{D}$  to construct the subspace affinity vector, which yields the normalized subspace affinity S. Subsequently, the refined subspace affinity  $\hat{S}$  is computed from S to provide self-supervised information. Then, we assign the corresponding patch-wise experts to the embedded representation  $\mathbf{z}$  according to S for modeling.

We only keep the real part of the result, and hence, we do not modify the feed-forward layers in the Transformer. The structure of the Frequency Encoder is depicted in Figure 2 (c), yielding frequency features  $z_f \in \mathbb{R}^{C \times N \times D}$ .

By modeling data in both the time and frequency domains, the DDE provides a more comprehensive understanding of temporal patterns, enabling the model to effectively handle complexities such as concept drift and evolving dynamics. This dual-domain perspective enhances the model's robustness and predictive accuracy, offering a versatile foundation for real-world time series forecasting.

#### 3.5 Pattern Identifier

To address the complex and evolving patterns in time series data, we introduce a novel Pattern Identifier (PI) module, an essential innovation within our framework. Unlike traditional approaches that treat the entire time series uniformly, our PI module dynamically classifies patches based on their distributional characteristics, enabling a more precise and adaptive modeling strategy.

The core of our approach lies in leveraging subspace clustering to detect concept shifts across multiple subspaces, as illustrated in Figure 3. The PI module plays a central role by directly analyzing the intrinsic properties of each patch and clustering them into distinct groups based on their latent patterns. In the time domain, PI enables TFPS to identify shifts in temporal characteristics such as seasonality and trends. In the frequency domain, it captures shifts associated with frequency-specific structures, like periodic behaviors and spectral changes, providing a comprehensive perspective on evolving patterns throughout the series.

To provide clarity, Figure 3 showcases an application of the PI module exclusively within the time domain. However, the insights and methodology seamlessly extend to the frequency domain, presenting a unified solution to the challenge of concept shifts.

The PI module iteratively refines subspace bases, which in turn improve representation learning and enable more accurate modeling of evolving patterns. It operates through the following three steps.

**Construction of Subspace Bases.** We define a new variable  $\mathbf{D} = [\mathbf{D}^{(1)}, \mathbf{D}^{(2)}, \cdots, \mathbf{D}^{(K)}]$  to represent the bases of K subspaces, where  $\mathbf{D}$  consists of K blocks, each  $\mathbf{D}^{(j)} \in \mathbf{R}^{q \times d}$ ,  $\|\mathbf{D}_u^{(j)}\| = 1, u = 1, \cdots, d, j = 1, \cdots, K$ . To control the column sizes of  $\mathbf{D}$ , we impose the following constraint:

$$R_1 = \frac{1}{2} \left\| \mathbf{D}^T \mathbf{D} \odot \mathbf{I} - \mathbf{I} \right\|_F^2, \tag{3}$$

where  $\odot$  denotes the Hadamard product, and I is an identity matrix of size  $Kd \times Kd$ .

**Subspaces Differentiation.** To ensure the dissimilarity between different subspaces, we introduce the second constraint:

$$R_{2} = \frac{1}{2} \left\| \mathbf{D}^{(j)T} \mathbf{D}^{(l)} \right\|_{F}^{2}, \quad j \neq l,$$

$$= \frac{1}{2} \left\| \mathbf{D}^{T} \mathbf{D} \odot \mathbf{O} \right\|_{F}^{2},$$
(4)

where O is a matrix with all off-diagonal d-size blocks set to 1 and diagonal blocks set to 0. Combining  $R_1$  and  $R_2$  yields the regularization term for R:

$$R = \alpha (R_1 + R_2),\tag{5}$$

where  $\alpha$  is a tuning parameters, fixed at  $10^{-3}$  in this work.

**Subspace Affinity and Refinement.** We propose a novel subspace affinity measure S to assess the relationship between the embedded representation z from DDE and the subspace bases D. The affinity  $s_{ij}$ , representing the probability that the embedded  $\mathbf{z}_i$  belongs to the j-th subspace, is defined as:

$$s_{ij} = \frac{\left\|\mathbf{z}_i^T \mathbf{D}^{(j)}\right\|_F^2 + \eta d}{\sum_j (\left\|\mathbf{z}_i^T \mathbf{D}^{(j)}\right\|_F^2 + \eta d)},\tag{6}$$

where  $\eta$  is a parameter controlling the smoothness, fixed to the same value as d. To emphasize more confident assignments, we introduce a refined subspace affinity  $\hat{s}_{ij}$ :

$$\hat{s}_{ij} = \frac{s_{ij}^2 / \sum_i s_{ij}}{\sum_j (s_{ij}^2 / \sum_i s_{ij})}.$$
 (7)

This refinement sharpens the clustering by weighting high-confidence assignments more. The subspace clustering objective based on the Kullback-Leibler divergence is:

$$\mathcal{L}_{sub} = KL(\hat{S} \parallel S) = \sum_{i} \sum_{j} \hat{s}_{ij} log \frac{\hat{s}_{ij}}{s_{ij}}.$$
 (8)

The clustering loss is defined as:

$$\mathcal{L}_{PI} = R + \beta \mathcal{L}_{sub},\tag{9}$$

where  $\beta$  is a hyperparameter balancing the regularization and subspace clustering terms. A detailed sensitivity analysis of  $\alpha$  and  $\beta$  is presented in Appendix J.

# 3.6 Mixture of Pattern Experts

Traditional time series forecasting methods often rely on a uniform distribution modeling (UDM) approach, which struggles to adapt to the complexities of diverse and evolving patterns in real-world data. To address this limitation, we introduce the Mixture of Pattern Experts module (MoPE), which assigns specialized experts to patches based on their unique underlying patterns, enabling more precise and adaptive forecasting.

Given the cluster assignments s obtained from the PI module, we apply the Patch-wise MoPE to the feature tensor  $z \in \mathbb{R}^{C \times N \times D}$ . The MoPE module consists of the following key components:

Gating Network. The gating network G calculates the gating weights for each expert based on the cluster assignment s and selects the top k experts. The gating weights are computed as:

$$G(s) = \text{Softmax}(\text{TopK}(s)). \tag{10}$$

Here, the top k logits are selected and normalized using the Softmax function to produce the gating weights.

**Expert Networks.** The MoPE contains K expert networks, denoted as  $E_1, \ldots, E_K$ . Each expert network is modeled as an MLP consisting of two linear layers and a ReLU activation. Given a patch-wise feature z, each expert network  $E_k$  processes the input to generate its respective output.

**Output Aggregation.** The final output h of the MoPE module is a weighted sum of the outputs from all the selected experts, with the weights provided by the gating network:

$$h = \sum_{k=1}^{K} G(s)E_k(z). \tag{11}$$

After the frequency branch is processed by the inverse Fast Fourier transform, the time-frequency outputs  $h_t$  and  $h_f$ , are concatenated to form  $h = \text{concat}(h_t, h_f) \in \mathbb{R}^{C \times N \times 2D}$ .

Finally, a linear transformation is applied to the disentangled and pattern-specific representations h to generate the prediction:  $\hat{Y} = \text{Linear}(h) \in \mathbb{R}^{H \times C}$ .

This approach ensures that the MoPE dynamically assigns and aggregates contributions from various experts based on evolving patterns, improving the model's adaptability and accuracy.

#### 3.7 Loss Function

Following [44], we use the Mean Squared Error (MSE) loss to quantify the discrepancy between predicted values  $\hat{Y}$  and ground truth values Y:  $\mathcal{L}_{MSE} = (\hat{Y} - Y)^2$ . In addition to the MSE loss, we incorporate the clustering regularization loss from the PI module, yielding the final loss function:

$$\mathcal{L} = \mathcal{L}_{MSE} + \mathcal{L}_{PI_t} + \mathcal{L}_{PI_f}. \tag{12}$$

This combined loss ensures that the model not only minimizes forecasting errors but also accurately identifies and maintains the integrity of pattern clusters across time. The algorithm is provided in the Appendix L.

# 4 Experiments

#### 4.1 Experimental Setup

**Datasets and Baselines.** We conducted our experiments on nine publicly available real-world multivariate time series datasets, i.e., ETT (ETTh1, ETTh2, ETTm1, ETTm2), Exchange, Weather, Electricity, Traffic, and ILI. These datasets are provided in [62] for time series forecasting. More details about these datasets are included in Appendix A.

We employed a diverse set of state-of-the-art forecasting models as baselines, categorized based on the type of information they utilize as follows. (1) **Time-domain methods:** PatchTST [44], DLinear [69], TimesNet [61] and iTransformer [29]; (2) **Frequency-domain methods:** FEDformer [71] and FITS [64]; (3) **Time-frequency methods:** TFDNet-IK [42] and TSLANet [9]. We rerun all the experiments with codes provided by their official implementation.

In addition, we compare TFPS with recent foundation models, including AutoTimes [30], Moment [16], and Timer [32]. We rerun all experiments for a fair comparison: AutoTimes is reproduced using its official implementation, while Moment and Timer are evaluated based on the OpenLTM [32].

We further include comparisons with normalization techniques, MoE-based architectures, and methods designed to address distribution shifts. Comprehensive results are presented in Appendix G.

**Experiments Details.** Following previous works [44], we used ADAM [21] as the default optimizer across all the experiments. We employed the MSE and mean absolute error (MAE) as the evaluation metrics, where lower values indicate better performance. A detailed explanation is provided in Appendix E. TFPS was implemented by PyTorch [48] and trained on a single NVIDIA RTX 3090 24GB GPU. We conducted grid search to optimize the following three parameters, i.e., learning rate =  $\{0.0001, 0.0005, 0.001, 0.005, 0.01, 0.005\}$ , the number of experts in the time domain  $K_t = \{1, 2, 4, 8\}$ , and the number of experts in the frequency domain  $K_f = \{1, 2, 4, 8\}$ .

#### 4.2 Overall Performance Comparison

Table 1 highlights the consistent superiority of TFPS across multiple datasets and prediction horizons, securing the top performance in 57 out of 72 experimental configurations. In particular, TFPS demonstrates significant improvements over time-domain methods, with an overall improvement of

Table 1: Multivariate long-term forecasting results with prediction lengths  $H \in \{24, 36, 48, 60\}$  for ILI and  $H \in \{96, 192, 336, 720\}$  for others. The input lengths are L = 104 for ILI and L = 96 for others. The best results are highlighted in **bold** and the second best are underlined.

M	odel	IMP.	TF (O		TSL		FI (20		iTrans (20		TFDN (20		Patch (20	nTST 23)		esNet (23)	DLi (20		FEDf	
M	etric	MSE	MSE	MAE	MSE	MAE	MSE	MAE	MSE	MAE	MSE	MAE	MSE	MAE	MSE	MAE	MSE	MAE	MSE	MAE
ETTh1	96 192 336 720	-1.1% 4.8% 1.8% 3.0%	0.398 0.423 0.484 0.488	0.413 0.423 0.461 0.476	0.387 0.448 0.491 0.505	0.405 0.436 0.487 0.486	0.395 0.445 0.489 0.496	0.403 0.432 0.463 0.485	$\begin{array}{c} \underline{0.387} \\ 0.441 \\ 0.491 \\ 0.509 \end{array}$	0.405 0.436 0.463 0.494	0.396 0.451 0.495 <u>0.492</u>	$0.409 \\ 0.441 \\ \underline{0.462} \\ \underline{0.482}$	0.413 0.460 0.497 0.501	0.419 0.445 0.463 0.486	0.389 0.441 0.491 0.512	0.412 0.442 0.467 0.491	0.398 0.434 0.499 0.508	0.410 0.427 0.477 0.503	0.385 0.441 0.491 0.501	0.425 0.461 0.473 0.499
ETTh2	96 192 336 720	-2.0% -2.9% 10.5% 12.6%	0.313 0.405 0.392 0.410	0.355 0.410 <b>0.415</b> <b>0.433</b>	$\begin{array}{c} \underline{0.290} \\ \underline{0.362} \\ \underline{0.401} \\ 0.419 \end{array}$	0.345 <b>0.391</b> <u>0.419</u> 0.439	0.295 0.382 0.416 <u>0.418</u>	0.344 0.396 0.425 <u>0.437</u>	0.301 0.380 0.424 0.430	0.350 0.399 0.432 0.447	0.289 0.379 0.416 0.424	0.337 0.395 0.422 0.441	0.299 0.383 0.424 0.429	0.348 0.398 0.431 0.445	0.324 0.393 0.429 0.433	0.368 0.410 0.437 0.448	0.315 0.432 0.486 0.732	0.374 0.447 0.481 0.614	0.342 0.434 0.512 0.467	0.383 0.440 0.497 0.476
ETTm1	96 192 336 720	4.1% 2.6% 4.2% -0.7%	0.327 0.374 0.401 0.479	0.367 0.395 0.408 0.456	0.329 0.376 0.403 0.445	$\begin{array}{c} \underline{0.368} \\ \underline{0.383} \\ 0.414 \\ \underline{0.438} \end{array}$	0.354 0.392 0.425 0.486	0.375 0.393 0.415 0.449	0.342 0.383 0.418 0.487	0.377 0.396 0.418 0.457	0.331 0.376 0.405 0.471	0.369 0.381 0.410 0.437	$\begin{array}{c} 0.331 \\ 0.374 \\ \hline 0.402 \\ \hline 0.466 \end{array}$	0.370 0.395 0.412 0.446	0.337 0.395 0.433 0.484	0.377 0.406 0.432 0.458	0.346 0.382 0.414 0.478	0.374 0.392 0.414 0.455	0.360 0.395 0.448 0.491	0.406 0.427 0.458 0.479
ETTm2	96 192 336 720	6.9% 7.1% 4.6% 3.6%	0.170 0.235 0.297 0.401	0.255 0.296 0.335 0.397	0.179 0.243 0.308 0.403	0.261 0.303 0.345 0.400	0.183 0.247 0.307 0.407	0.266 0.305 0.342 0.401	0.186 0.254 0.316 0.414	0.272 0.314 0.351 0.407	$\begin{array}{c} \frac{0.176}{0.245} \\ \frac{0.303}{0.405} \end{array}$	$0.267 \\ \underline{0.302} \\ \underline{0.340} \\ \underline{0.399}$	0.177 0.248 0.303 0.405	0.260 0.306 0.341 0.403	0.182 0.252 0.312 0.417	0.262 0.307 0.346 0.404	0.184 0.282 0.324 0.441	0.276 0.357 0.364 0.454	0.193 0.256 0.321 0.434	0.285 0.324 0.364 0.426
Exchange	96 192 336 720	12.7% 11.2% 10.4% -13.3%	0.083 0.174 0.310 1.011	0.205 0.297 0.398 0.756	0.085 0.178 0.329 0.850	0.206 0.300 0.415 0.693	0.088 0.181 0.324 0.846	0.210 0.304 0.413 0.696	0.086 0.181 0.338 0.853	0.206 0.304 0.422 0.696	$ \begin{vmatrix} \frac{0.084}{0.176} \\ \hline{0.321} \\ \textbf{0.835} \end{vmatrix} $	0.205 0.299 0.409 <b>0.689</b>	0.089 0.178 0.326 0.840	0.206 0.302 0.411 0.690	0.105 0.219 0.353 0.912	0.233 0.342 0.433 0.724	$0.089 \\ 0.180 \\ \underline{0.313} \\ \underline{0.837}$	0.219 0.319 0.423 <u>0.690</u>	0.136 0.279 0.465 1.169	0.265 0.384 0.504 0.826
Weather	96 192 336 720	15.6% 10.6% 9.1% 4.1%	0.154 0.205 0.262 0.344	0.202 0.249 0.289 0.342	0.176 0.226 0.279 0.355	0.216 0.258 0.299 0.355	0.167 0.215 0.270 0.347	0.214 0.257 0.299 <u>0.345</u>	0.176 0.225 0.281 0.358	0.216 0.257 0.299 0.350	$\begin{array}{c} 0.165 \\ \hline 0.214 \\ \hline 0.267 \\ \hline 0.347 \\ \end{array}$	$\begin{array}{c} \underline{0.209} \\ \underline{0.252} \\ \underline{0.298} \\ 0.346 \end{array}$	0.177 0.225 0.278 0.351	0.219 0.259 0.298 0.346	0.168 0.226 0.283 0.355	0.218 0.267 0.305 0.353	0.197 0.237 0.283 0.347	0.257 0.294 0.332 0.382	0.236 0.268 0.366 0.407	0.325 0.337 0.402 0.422
Electricity	96 192 336 720	14.6% 12.0% 0.2% 7.2%	0.149 0.162 0.200 0.220	0.236 0.253 0.310 0.320	0.155 0.170 0.197 <u>0.224</u>	0.249 0.264 0.282 <u>0.318</u>	0.200 0.200 0.214 0.256	0.278 0.281 0.295 0.328	$\begin{array}{c} \underline{0.151} \\ \underline{0.167} \\ \hline \textbf{0.179} \\ 0.229 \end{array}$	$\begin{array}{c} \underline{0.241} \\ \underline{0.258} \\ \hline \textbf{0.271} \\ 0.319 \end{array}$	0.171 0.189 0.205 0.247	0.254 0.269 0.284 0.318	0.166 0.174 0.190 0.230	0.252 0.261 <u>0.277</u> <b>0.312</b>	0.168 0.186 0.197 0.225	0.272 0.289 0.298 0.322	0.195 0.194 0.207 0.243	0.277 0.281 0.296 0.330	0.189 0.198 0.212 0.242	0.304 0.312 0.326 0.351
Traffic	96 192 336 720	21.1% 17.7% 17.0% 15.1%	0.427 0.445 0.459 0.496	0.296 0.298 0.307 0.313	0.475 0.478 0.494 0.528	0.307 0.306 0.312 0.331	0.651 0.603 0.610 0.648	0.388 0.364 0.366 0.387	$\begin{array}{c} \underline{0.428} \\ \underline{0.448} \\ \underline{0.465} \\ \underline{0.501} \end{array}$	0.295 0.302 0.311 0.333	0.519 0.513 0.525 0.561	0.314 0.314 0.319 0.336	0.446 0.453 0.467 0.501	0.284 0.285 0.291 0.492	0.586 0.618 0.634 0.659	0.316 0.323 0.337 0.349	0.650 0.600 0.606 0.646	0.397 0.372 0.374 0.396	0.575 0.613 0.622 0.630	0.357 0.381 0.380 0.383
II	24 36 48 60	40.9% 43.6% 40.4% 39.8%	1.349 1.239 1.461 1.458	0.760 0.752 0.801 0.836	1.749 1.754 2.050 2.240	0.898 0.912 0.984 1.039	3.489 3.530 3.671 4.030	1.373 1.370 1.391 1.462	2.443 2.455 3.437 2.734	1.078 1.086 1.331 1.155	1.824 1.699 1.762 1.758	$\begin{array}{c} \underline{0.824} \\ \underline{0.813} \\ \underline{0.831} \\ \underline{0.863} \end{array}$	$\begin{array}{r} \underline{1.614} \\ \underline{1.475} \\ \underline{1.642} \\ \underline{1.608} \end{array}$	0.835 0.859 0.880 0.885	1.699 1.733 2.272 1.998	0.871 0.913 0.999 0.974	2.239 2.238 2.252 2.236	1.041 1.049 1.064 1.057	3.217 2.688 2.540 2.782	1.246 1.074 1.057 1.136
	1st C	ount	5	7	3	3	1	1	3	3	(	5		1	(	)	(	)	1	1

Table 2: Ablation study of TFPS components. The model variants in our ablation study include the following configurations across both time and frequency branches: (a) inclusion of the encoder, PI and MoPE; (b) PI replaced with Linear; (c) only the encoder. The best results are in **bold**.

Tiı	ne Brancl	h	Frequ	iency Bra	nch	ET	Th1		ET	Th2	
Encoder	PI	MoPE	Encoder	PI	MoPE   96	192	336	720   96	192	336	720
✓	✓	✓	✓	✓	√   0.398	0.423	0.484	0.488   0.313	0.405	0.392	0.410
√ √ √	√ Linear	√ √			$ \begin{vmatrix}     0.401 \\     0.401 \\     0.414 \end{vmatrix} $	$0.459 \\ \underline{0.451} \\ 0.460$	0.486 0.494 0.501	$\begin{array}{c c} 0.492 \\ \hline 0.509 \\ 0.500 \end{array} \begin{vmatrix} 0.318 \\ 0.325 \\ 0.500 \end{vmatrix}$	0.409 0.411 0.411	0.400 0.400 0.426	0.428 0.434 0.431
			√ √ √	√ Linear	✓ 0.455 ✓ 0.503 0.552	0.507 0.535 0.583	0.539 0.558 0.591	0.576         0.324           0.583         0.398           0.594         0.371	0.407 0.446 0.426	0.417 0.457 0.418	0.436 0.444 0.463

9.5% in MSE and 6.4% in MAE. Compared to frequency-domain methods, TFPS shows even more pronounced enhancements, with MSE improved by 16.9% and MAE by 12.4%.

While the time-frequency methods like TSLANet and TFDNet perform competitively on several datasets, TFPS still outperforms them, showing improvement of 5.2% in MSE and 2.2% in MAE. These substantial improvements can be attributed to the integration of both time- and frequency-domain information, combined with our innovative approach to modeling distinct patterns with specialized experts. By addressing the underlying concept shifts and capturing complex, evolving patterns in time series data, TFPS achieves more accurate predictions than other baselines.

Table 3: Compared with foundation models.

Model	IMP.		PS ur)		Times (24)		ment 024)		ner (24)
Metric	MSE	MSE	MAE	MSE	MAE	MSE	MAE	MSE	MAE
ETTh1 ETTh2 ETTm1 ETTm2 Traffic	0.2% 10.9% 2.4% 7.3% -3.6%	0.401 0.335 0.343 0.248 0.398	0.412 0.386 0.374 0.308 0.268	0.396 0.363 0.364 0.273 0.379	0.428 0.406 0.389 0.327 0.265	0.415 0.381 0.348 0.265 0.395	0.439 0.412 0.386 0.325 0.273	0.394 0.382 0.344 0.264 0.379	0.417 0.418 0.378 0.321 0.255
Electricity	3.7%	0.159	0.249	0.168	0.261	0.163	0.263	0.165	0.258

Table 4: Compared with normalization methods.

Model	IMP.	D	Linear			
			SIN	SAN	Dish-TS	RevIN
ETTh1	1.5%	0.448	0.454	0.456	0.461	0.451
ETTh2	2.4%	0.380	0.386	0.388	0.392	0.390
ETTm1	2.3%	0.395	0.405	0.399	0.406	0.409
ETTm2	3.3%	0.276	0.283	0.280	0.293	0.284
Weather	5.3%	0.241	0.253	0.249	0.263	0.254

#### 4.3 Ablation Study

Table 2 presents the MSE results of TFPS and its variants with different combinations of encoders, PI, and MoPE. 1) Best Result. The full TFPS model, i.e., both the time and frequency branches, along with their respective encoders, PI, and MoPE are included, performs the best across all the forecast horizons for both datasets. 2) Linear vs. PI. We replace PI with a linear layer and find that it generally results in higher MSE in most cases, indicating that accurately capturing specific patterns is crucial. 3) Impact of Pattern-aware Modeling. Additionally, when comparing the results with the encoder-only configuration, two variants with MoPE in each branch achieved improved MSE, further supporting the necessity of patter-aware modeling. 4) Importance of DDE. Furthermore, we find that both the time encoder and frequency encoder alone yield worse performance, with the time encoder playing a more significant role. In summary, incorporating both branches with PI and MoPE provides the best performance, while simpler configurations result in higher MSE. See Appendix K for an in-depth analysis of each component's contribution.

## 4.4 Comparsion with Foundation Models

To ensure a fair comparison with foundation models, we searched input lengths among 96, 192, 336, and 512. The average results across all forecasting lengths are included in Table 3, with detailed results provided in Appendix F.2. As shown in Table 3, TFPS consistently outperforms recent foundation models. Notably, on challenging datasets such as ETTh2 and ETTm2, TFPS achieves substantial improvements in MSE by 10.9% and 7.3%, respectively. Although TFPS performs slightly worse on the Traffic dataset, we attribute this to the relatively mild distribution shift observed in Traffic (see Table 5), which may reduce the benefit of our pattern-specific modeling. These results suggest that TFPS not only matches but often surpasses large-scale foundation models in forecasting accuracy, benefiting from its expert-based design that explicitly captures distributional heterogeneity.

#### 4.5 Comparsion with Normalization Methods

Normalization methods can reduce fluctuations to enhance performance and are widely used for non-stationary time series forecasting [17, 34, 10, 31, 20]. We compare our TFPS with these state-of-the-art normalization methods and Table 4 presents the average MSE across all forecasting lengths for each dataset. While normalization improves stability by enforcing distributional consistency, TFPS retains the intrinsic non-stationarity and models diverse patterns through distribution-specific experts, achieving better adaptability and forecasting accuracy. Detailed results are provided in Appendix G.1.

#### 4.6 Visualization

We visualize the prediction curves for ETTh1 with H=192. Given that DLinear exhibits competitive performance in Table 1, we compare its results with those of TFPS in Figure 4 under two scenarios: (a) sudden drift caused by external factors or random events, and (b) gradual drift where the trend is dominant. It is evident that DLinear struggles to achieve accurate predictions in both scenarios. In contrast, our TFPS consistently produces accurate forecasts despite these challenges, demonstrating its robustness in dealing with various concept dynamics.

#### 4.7 Analysis of Experts

**Qualitative Visualizations of Pattern Identifier.** Through training, pattern experts in MoPE spontaneously specialize, and we present two examples in Figure 5. We visualize the expert with the highest score as the routed expert for each instance pair. In the provided examples, we observe that

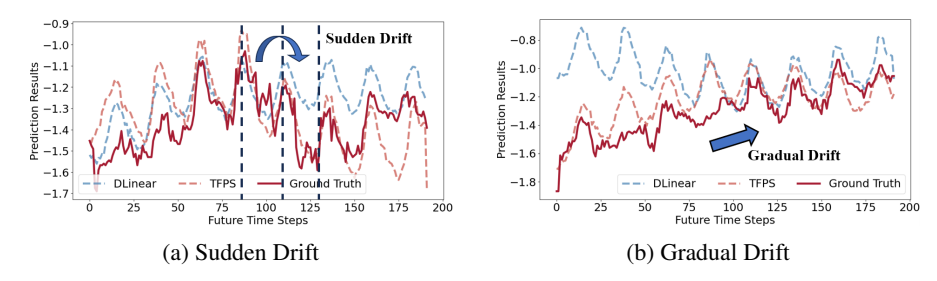


Figure 4: Visualizations of DLinear and TFPS on the ETTh1 dataset when H = 192.

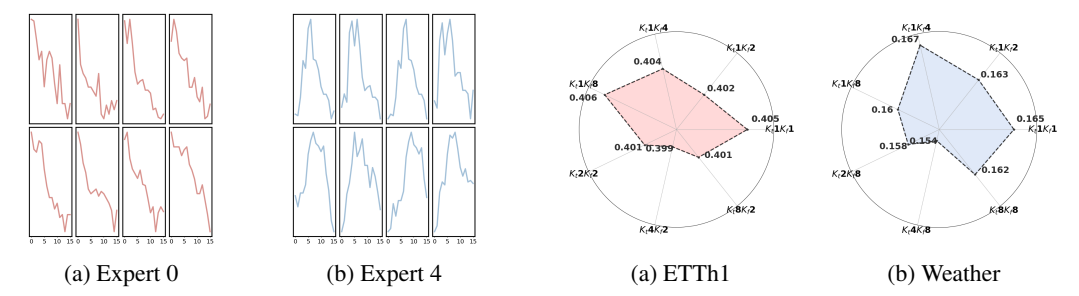


Figure 5: Interpretable patterns via PI. Expert-0 specializes in downward trends, while Expert-4 focuses on parabolic trends.

Figure 6: Experiments on the number of experts when H=96. Further analysis of expert behavior is provided in Appendix H.

expert-0 specialize in downward-related concepts, while expert-4 focuses on parabolic trend. These examples also demonstrate the interpretability of MoPE.

**Number of Experts.** In Figure 6, we set the learning rate to 0.0001 and conducted four sets of experiments on the ETTh1 and Weather datasets,  $K_t = 1$ ,  $K_f = \{1, 2, 4, 8\}$ , to explore the effect of the number of frequency experts on the results. For example,  $K_t 1 K_f 4$  means that the TFPS contains 1 time experts and 4 frequency experts. We observed that  $K_t 1 K_f 2$  outperformed  $K_t 1 K_f 4$  in both cases, suggesting that increasing the number of experts does not always lead to better performance.

In addition, we conducted three experiments based on the optimal number of frequency experts to verify the impact of varying the number of time experts on the results. As shown in Figure 6, the best results for ETTh1 were obtained with  $K_t 4K_f 2$ , while for Weather, the optimal results were achieved with  $K_t 4K_f 8$ . Combined with the average Wasserstein distance in Table 5, we attribute this to the fact that, in cases where concept drift is more severe, such as Weather, more experts are needed, whereas fewer experts are sufficient when the drift is less severe.

# 5 Conclusion

In this paper, we propose a novel pattern-aware time series forecasting framework, TFPS, which incorporates a dual-domain mixture of pattern experts approach. Our TFPS framework aims to address the distribution shift across time series patches and effectively assigns pattern-specific experts to model them. Experimental results across eight diverse datasets demonstrate that TFPS surpasses state-of-the-art methods in both quantitative metrics and visualizations. Future work will focus on investigating evolving distribution shifts, particularly those introduced by the emergence of new patterns, such as unforeseen epidemics or outbreaks.

# 6 Acknowledgments and Disclosure of Funding

This work was supported in part by the National Natural Science Foundation of China under Grants U23B2049, 62376194, 61925602, 62406219, and 62436001; in part by the China Postdoctoral Science Foundation - Tianjin Joint Support Program under Grant 2023T014TJ; and in part by the China Scholarship Council under Grant 202406250137.

#### References

- [1] Khaled Alkilane, Yihang He, and Der-Horng Lee. Mixmamba: Time series modeling with adaptive expertise. *Information Fusion*, 112:102589, 2024.
- [2] Quentin Gregory Anthony, Yury Tokpanov, Paolo Glorioso, and Beren Millidge. Blackmamba: Mixture of experts for state-space models. In *ICLR 2024 Workshop on Mathematical and Empirical Understanding of Foundation Models*, 2024.
- [3] Kaifeng Bi, Lingxi Xie, Hengheng Zhang, Xin Chen, Xiaotao Gu, and Qi Tian. Accurate medium-range global weather forecasting with 3d neural networks. *Nature*, 619(7970):533–538, 2023.
- [4] Yushu Chen, Shengzhuo Liu, Jinzhe Yang, Hao Jing, Wenlai Zhao, and Guangwen Yang. A joint time-frequency domain transformer for multivariate time series forecasting. *Neural Networks*, 176:106334, 2024.
- [5] Damai Dai, Chengqi Deng, Chenggang Zhao, RX Xu, Huazuo Gao, Deli Chen, Jiashi Li, Wangding Zeng, Xingkai Yu, Y Wu, et al. Deepseekmoe: Towards ultimate expert specialization in mixture-of-experts language models. *arXiv preprint arXiv:2401.06066*, 2024.
- [6] Jacob Devlin, Ming-Wei Chang, Kenton Lee, and Kristina Toutanova. Bert: Pre-training of deep bidirectional transformers for language understanding. In *Proceedings of the 2019 conference of the North American chapter of the association for computational linguistics: human language technologies, volume 1 (long and short papers)*, pages 4171–4186, 2019.
- [7] Nan Du, Yanping Huang, Andrew M Dai, Simon Tong, Dmitry Lepikhin, Yuanzhong Xu, Maxim Krikun, Yanqi Zhou, Adams Wei Yu, Orhan Firat, et al. Glam: Efficient scaling of language models with mixture-of-experts. In *International Conference on Machine Learning*, pages 5547–5569. PMLR, 2022.
- [8] Vijay Ekambaram, Arindam Jati, Nam Nguyen, Phanwadee Sinthong, and Jayant Kalagnanam. Tsmixer: Lightweight mlp-mixer model for multivariate time series forecasting. In *Proceedings of the 29th ACM SIGKDD Conference on Knowledge Discovery and Data Mining*, pages 459–469, 2023.
- [9] Emadeldeen Eldele, Mohamed Ragab, Zhenghua Chen, Min Wu, and Xiaoli Li. TSLANet: Rethinking transformers for time series representation learning. In *Forty-first International Conference on Machine Learning*, 2024.
- [10] Wei Fan, Pengyang Wang, Dongkun Wang, Dongjie Wang, Yuanchun Zhou, and Yanjie Fu. Dish-ts: a general paradigm for alleviating distribution shift in time series forecasting. In Proceedings of the AAAI conference on artificial intelligence, volume 37, pages 7522–7529, 2023.
- [11] Wei Fan, Shun Zheng, Pengyang Wang, Rui Xie, Jiang Bian, and Yanjie Fu. Addressing distribution shift in time series forecasting with instance normalization flows. *arXiv* preprint *arXiv*:2401.16777, 2024.
- [12] William Fedus, Barret Zoph, and Noam Shazeer. Switch transformers: Scaling to trillion parameter models with simple and efficient sparsity. *Journal of Machine Learning Research*, 23(120):1–39, 2022.
- [13] Yunpeng Gong, Liqing Huang, and Lifei Chen. Eliminate deviation with deviation for data augmentation and a general multi-modal data learning method. *arXiv preprint arXiv:2101.08533*, 2021.
- [14] Yunpeng Gong, Liqing Huang, and Lifei Chen. Person re-identification method based on color attack and joint defence. In *Proceedings of the IEEE/CVF conference on computer vision and pattern recognition*, pages 4313–4322, 2022.
- [15] Yunpeng Gong, Zhun Zhong, Yansong Qu, Zhiming Luo, Rongrong Ji, and Min Jiang. Cross-modality perturbation synergy attack for person re-identification. Advances in Neural Information Processing Systems, 37:23352–23377, 2024.

- [16] Mononito Goswami, Konrad Szafer, Arjun Choudhry, Yifu Cai, Shuo Li, and Artur Dubrawski. Moment: A family of open time-series foundation models. In *International Conference on Machine Learning*, pages 16115–16152. PMLR, 2024.
- [17] Lu Han, Han-Jia Ye, and De-Chuan Zhan. SIN: Selective and interpretable normalization for long-term time series forecasting. In *Forty-first International Conference on Machine Learning*, 2024.
- [18] Hongbin Huang, Minghua Chen, and Xiao Qiao. Generative learning for financial time series with irregular and scale-invariant patterns. In *The Twelfth International Conference on Learning Representations*, 2024.
- [19] Yushan Jiang, Kanghui Ning, Zijie Pan, Xuyang Shen, Jingchao Ni, Wenchao Yu, Anderson Schneider, Haifeng Chen, Yuriy Nevmyvaka, and Dongjin Song. Multi-modal time series analysis: A tutorial and survey. In *Proceedings of the 31st ACM SIGKDD Conference on Knowledge Discovery and Data Mining V. 2*, pages 6043–6053, 2025.
- [20] Taesung Kim, Jinhee Kim, Yunwon Tae, Cheonbok Park, Jang-Ho Choi, and Jaegul Choo. Reversible instance normalization for accurate time-series forecasting against distribution shift. In *International Conference on Learning Representations*, 2021.
- [21] Diederik P Kingma and Jimmy Ba. Adam: A method for stochastic optimization. arXiv preprint arXiv:1412.6980, 2014.
- [22] Weiyang Kong, Ziyu Guo, and Yubao Liu. Spatio-temporal pivotal graph neural networks for traffic flow forecasting. In *Proceedings of the AAAI Conference on Artificial Intelligence*, volume 38, pages 8627–8635, 2024.
- [23] Guokun Lai, Wei-Cheng Chang, Yiming Yang, and Hanxiao Liu. Modeling long-and short-term temporal patterns with deep neural networks. In *The 41st international ACM SIGIR conference on research & development in information retrieval*, pages 95–104, 2018.
- [24] Remi Lam, Alvaro Sanchez-Gonzalez, Matthew Willson, Peter Wirnsberger, Meire Fortunato, Ferran Alet, Suman Ravuri, Timo Ewalds, Zach Eaton-Rosen, Weihua Hu, et al. Learning skillful medium-range global weather forecasting. *Science*, 382(6677):1416–1421, 2023.
- [25] Sanghyun Lee and Chanyoung Park. Continual traffic forecasting via mixture of experts. *arXiv* preprint arXiv:2406.03140, 2024.
- [26] James Lee-Thorp, Joshua Ainslie, Ilya Eckstein, and Santiago Ontanon. Fnet: Mixing tokens with fourier transforms. In *Proceedings of the 2022 Conference of the North American Chapter of the Association for Computational Linguistics: Human Language Technologies*, pages 4296–4313, 2022.
- [27] Zhe Li, Shiyi Qi, Yiduo Li, and Zenglin Xu. Revisiting long-term time series forecasting: An investigation on linear mapping. *arXiv preprint arXiv:2305.10721*, 2023.
- [28] Xvyuan Liu, Xiangfei Qiu, Xingjian Wu, Zhengyu Li, Chenjuan Guo, Jilin Hu, and Bin Yang. Rethinking irregular time series forecasting: A simple yet effective baseline. *arXiv* preprint *arXiv*:2505.11250, 2025.
- [29] Yong Liu, Tengge Hu, Haoran Zhang, Haixu Wu, Shiyu Wang, Lintao Ma, and Mingsheng Long. itransformer: Inverted transformers are effective for time series forecasting. In *The Twelfth International Conference on Learning Representations*, 2024.
- [30] Yong Liu, Guo Qin, Xiangdong Huang, Jianmin Wang, and Mingsheng Long. Autotimes: Autoregressive time series forecasters via large language models. *Advances in Neural Information Processing Systems*, 37:122154–122184, 2024.
- [31] Yong Liu, Haixu Wu, Jianmin Wang, and Mingsheng Long. Non-stationary transformers: Exploring the stationarity in time series forecasting. *Advances in Neural Information Processing Systems*, 35:9881–9893, 2022.

- [32] Yong Liu, Haoran Zhang, Chenyu Li, Xiangdong Huang, Jianmin Wang, and Mingsheng Long. Timer: generative pre-trained transformers are large time series models. In *Proceedings of the 41st International Conference on Machine Learning*, pages 32369–32399, 2024.
- [33] Zhanyu Liu, Guanjie Zheng, and Yanwei Yu. Cross-city few-shot traffic forecasting via traffic pattern bank. In *Proceedings of the 32nd ACM International Conference on Information and Knowledge Management*, pages 1451–1460, 2023.
- [34] Zhiding Liu, Mingyue Cheng, Zhi Li, Zhenya Huang, Qi Liu, Yanhu Xie, and Enhong Chen. Adaptive normalization for non-stationary time series forecasting: A temporal slice perspective. *Advances in Neural Information Processing Systems*, 36, 2023.
- [35] Qingqing Long, Zheng Fang, Chen Fang, Chong Chen, Pengfei Wang, and Yuanchun Zhou. Unveiling delay effects in traffic forecasting: A perspective from spatial-temporal delay differential equations. In *Proceedings of the ACM on Web Conference 2024*, pages 1035–1044, 2024.
- [36] Jie Lu, Anjin Liu, Fan Dong, Feng Gu, Joao Gama, and Guangquan Zhang. Learning under concept drift: A review. *IEEE transactions on knowledge and data engineering*, 31(12):2346– 2363, 2018.
- [37] Shilin Lu, Zhuming Lian, Zihan Zhou, Shaocong Zhang, Chen Zhao, and Adams Wai-Kin Kong. Does flux already know how to perform physically plausible image composition? *arXiv* preprint arXiv:2509.21278, 2025.
- [38] Shilin Lu, Yanzhu Liu, and Adams Wai-Kin Kong. Tf-icon: Diffusion-based training-free cross-domain image composition. In *Proceedings of the IEEE/CVF International Conference* on Computer Vision, pages 2294–2305, 2023.
- [39] Shilin Lu, Zilan Wang, Leyang Li, Yanzhu Liu, and Adams Wai-Kin Kong. Mace: Mass concept erasure in diffusion models. In *Proceedings of the IEEE/CVF Conference on Computer Vision and Pattern Recognition*, pages 6430–6440, 2024.
- [40] Shilin Lu, Zihan Zhou, Jiayou Lu, Yuanzhi Zhu, and Adams Wai-Kin Kong. Robust water-marking using generative priors against image editing: From benchmarking to advances. *arXiv* preprint arXiv:2410.18775, 2024.
- [41] Donghao Luo and Xue Wang. Moderntcn: A modern pure convolution structure for general time series analysis. In *The Twelfth International Conference on Learning Representations*, 2024.
- [42] Yuxiao Luo, Ziyu Lyu, and Xingyu Huang. Tfdnet: Time-frequency enhanced decomposed network for long-term time series forecasting. *arXiv preprint arXiv:2308.13386*, 2023.
- [43] Ronghao Ni, Zinan Lin, Shuaiqi Wang, and Giulia Fanti. Mixture-of-linear-experts for long-term time series forecasting. In *International Conference on Artificial Intelligence and Statistics*, pages 4672–4680. PMLR, 2024.
- [44] Yuqi Nie, Nam H Nguyen, Phanwadee Sinthong, and Jayant Kalagnanam. A time series is worth 64 words: Long-term forecasting with transformers. In *The Eleventh International Conference on Learning Representations*, 2023.
- [45] Kanghui Ning, Zijie Pan, Yu Liu, Yushan Jiang, James Y Zhang, Kashif Rasul, Anderson Schneider, Lintao Ma, Yuriy Nevmyvaka, and Dongjin Song. Ts-rag: Retrieval-augmented generation based time series foundation models are stronger zero-shot forecaster. *arXiv preprint arXiv:2503.07649*, 2025.
- [46] Eduardo Ogasawara, Leonardo C Martinez, Daniel De Oliveira, Geraldo Zimbrão, Gisele L Pappa, and Marta Mattoso. Adaptive normalization: A novel data normalization approach for non-stationary time series. In *The 2010 International Joint Conference on Neural Networks (IJCNN)*, pages 1–8. IEEE, 2010.
- [47] Nikolaos Passalis, Anastasios Tefas, Juho Kanniainen, Moncef Gabbouj, and Alexandros Iosifidis. Deep adaptive input normalization for time series forecasting. *IEEE transactions on neural networks and learning systems*, 31(9):3760–3765, 2019.

- [48] Adam Paszke, Sam Gross, Francisco Massa, Adam Lerer, James Bradbury, Gregory Chanan, Trevor Killeen, Zeming Lin, Natalia Gimelshein, Luca Antiga, et al. Pytorch: An imperative style, high-performance deep learning library. *Advances in neural information processing systems*, 32, 2019.
- [49] Maciej Pióro, Kamil Ciebiera, Krystian Król, Jan Ludziejewski, Michał Krutul, Jakub Krajewski, Szymon Antoniak, Piotr Miłoś, Marek Cygan, and Sebastian Jaszczur. Moe-mamba: Efficient selective state space models with mixture of experts. In *ICLR 2024 Workshop on Mathematical and Empirical Understanding of Foundation Models*, 2024.
- [50] Joan Puigcerver, Carlos Riquelme, Basil Mustafa, and Neil Houlsby. From sparse to soft mixtures of experts. *arXiv preprint arXiv:2308.00951*, 2023.
- [51] Xiangfei Qiu, Jilin Hu, Lekui Zhou, Xingjian Wu, Junyang Du, Buang Zhang, Chenjuan Guo, Aoying Zhou, Christian S. Jensen, Zhenli Sheng, and Bin Yang. Tfb: Towards comprehensive and fair benchmarking of time series forecasting methods. *Proc. VLDB Endow.*, 17(9):2363–2377, 2024.
- [52] Xiangfei Qiu, Xingjian Wu, Yan Lin, Chenjuan Guo, Jilin Hu, and Bin Yang. Duet: Dual clustering enhanced multivariate time series forecasting. In *Proceedings of the 31st ACM SIGKDD Conference on Knowledge Discovery and Data Mining*, pages 1185–1196, 2025.
- [53] Xiangfei Qiu, Yuhan Zhu, Zhengyu Li, Hanyin Cheng, Xingjian Wu, Chenjuan Guo, Bin Yang, and Jilin Hu. Dag: A dual causal network for time series forecasting with exogenous variables. arXiv preprint arXiv:2509.14933, 2025.
- [54] Aaditya Ramdas, Nicolás García Trillos, and Marco Cuturi. On wasserstein two-sample testing and related families of nonparametric tests. *Entropy*, 19(2):47, 2017.
- [55] Artsiom Sanakoyeu, Vadim Tschernezki, Uta Buchler, and Bjorn Ommer. Divide and conquer the embedding space for metric learning. In *Proceedings of the ieee/cvf conference on computer vision and pattern recognition*, pages 471–480, 2019.
- [56] Zezhi Shao, Fei Wang, Yongjun Xu, Wei Wei, Chengqing Yu, Zhao Zhang, Di Yao, Tao Sun, Guangyin Jin, Xin Cao, et al. Exploring progress in multivariate time series forecasting: Comprehensive benchmarking and heterogeneity analysis. *IEEE Transactions on Knowledge and Data Engineering*, 2024.
- [57] Noam Shazeer, \*Azalia Mirhoseini, \*Krzysztof Maziarz, Andy Davis, Quoc Le, Geoffrey Hinton, and Jeff Dean. Outrageously large neural networks: The sparsely-gated mixture-ofexperts layer. In *International Conference on Learning Representations*, 2017.
- [58] Ashish Vaswani, Noam Shazeer, Niki Parmar, Jakob Uszkoreit, Llion Jones, Aidan N Gomez, Łukasz Kaiser, and Illia Polosukhin. Attention is all you need. Advances in neural information processing systems, 30, 2017.
- [59] Hao Wang, Zhiyu Wang, Yunlong Niu, Zhaoran Liu, Haozhe Li, Yilin Liao, Yuxin Huang, and Xinggao Liu. An accurate and interpretable framework for trustworthy process monitoring. *IEEE Transactions on Artificial Intelligence*, 2023.
- [60] Qingsong Wen, Weiqi Chen, Liang Sun, Zhang Zhang, Liang Wang, Rong Jin, Tieniu Tan, et al. Onenet: Enhancing time series forecasting models under concept drift by online ensembling. *Advances in Neural Information Processing Systems*, 36:69949–69980, 2023.
- [61] Haixu Wu, Tengge Hu, Yong Liu, Hang Zhou, Jianmin Wang, and Mingsheng Long. Timesnet: Temporal 2d-variation modeling for general time series analysis. In *The Eleventh International Conference on Learning Representations*, 2023.
- [62] Haixu Wu, Jiehui Xu, Jianmin Wang, and Mingsheng Long. Autoformer: Decomposition transformers with auto-correlation for long-term series forecasting. *Advances in neural information processing systems*, 34:22419–22430, 2021.

- [63] Haixu Wu, Hang Zhou, Mingsheng Long, and Jianmin Wang. Interpretable weather forecasting for worldwide stations with a unified deep model. *Nature Machine Intelligence*, 5(6):602–611, 2023.
- [64] Zhijian Xu, Ailing Zeng, and Qiang Xu. FITS: Modeling time series with \$10k\$ parameters. In *The Twelfth International Conference on Learning Representations*, 2024.
- [65] Kaiwen Yan, Chen Long, Huisi Wu, and Zhenkun Wen. Multi-resolution expansion of analysis in time-frequency domain for time series forecasting. *IEEE Transactions on Knowledge and Data Engineering*, 2024.
- [66] Zhangjing Yang, Weiwu Yan, Xiaolin Huang, and Lin Mei. Adaptive temporal-frequency network for time-series forecasting. *IEEE Transactions on Knowledge and Data Engineering*, 34(4):1576–1587, 2020.
- [67] Chengqing Yu, Fei Wang, Zezhi Shao, Tangwen Qian, Zhao Zhang, Wei Wei, Zhulin An, Qi Wang, and Yongjun Xu. Ginar+: A robust end-to-end framework for multivariate time series forecasting with missing values. *IEEE Transactions on Knowledge and Data Engineering*, 2025.
- [68] Chengqing Yu, Fei Wang, Yilun Wang, Zezhi Shao, Tao Sun, Di Yao, and Yongjun Xu. Mgsf-former: A multi-granularity spatiotemporal fusion transformer for air quality prediction. *Information Fusion*, 113:102607, 2025.
- [69] Ailing Zeng, Muxi Chen, Lei Zhang, and Qiang Xu. Are transformers effective for time series forecasting? In *Proceedings of the AAAI conference on artificial intelligence*, volume 37, pages 11121–11128, 2023.
- [70] Haoyi Zhou, Shanghang Zhang, Jieqi Peng, Shuai Zhang, Jianxin Li, Hui Xiong, and Wancai Zhang. Informer: Beyond efficient transformer for long sequence time-series forecasting. In *Proceedings of the AAAI conference on artificial intelligence*, volume 35, pages 11106–11115, 2021.
- [71] Tian Zhou, Ziqing Ma, Qingsong Wen, Xue Wang, Liang Sun, and Rong Jin. Fedformer: Frequency enhanced decomposed transformer for long-term series forecasting. In *International conference on machine learning*, pages 27268–27286. PMLR, 2022.

# **NeurIPS Paper Checklist**

#### 1. Claims

Question: Do the main claims made in the abstract and introduction accurately reflect the paper's contributions and scope?

Answer: [Yes]

Justification: The main claims in the abstract and introduction accurately reflect the contributions and scope of the paper. They are supported by the proposed methodology, theoretical motivation, and extensive empirical results across diverse datasets.

#### Guidelines:

- The answer NA means that the abstract and introduction do not include the claims made in the paper.
- The abstract and/or introduction should clearly state the claims made, including the contributions made in the paper and important assumptions and limitations. A No or NA answer to this question will not be perceived well by the reviewers.
- The claims made should match theoretical and experimental results, and reflect how much the results can be expected to generalize to other settings.
- It is fine to include aspirational goals as motivation as long as it is clear that these goals
  are not attained by the paper.

#### 2. Limitations

Question: Does the paper discuss the limitations of the work performed by the authors?

Answer: [Yes]

Justification: The paper discusses the limitations of the proposed method in Section N, including its assumptions about fixed patch length and potential challenges under evolving distributions.

#### Guidelines:

- The answer NA means that the paper has no limitation while the answer No means that the paper has limitations, but those are not discussed in the paper.
- The authors are encouraged to create a separate "Limitations" section in their paper.
- The paper should point out any strong assumptions and how robust the results are to violations of these assumptions (e.g., independence assumptions, noiseless settings, model well-specification, asymptotic approximations only holding locally). The authors should reflect on how these assumptions might be violated in practice and what the implications would be.
- The authors should reflect on the scope of the claims made, e.g., if the approach was only tested on a few datasets or with a few runs. In general, empirical results often depend on implicit assumptions, which should be articulated.
- The authors should reflect on the factors that influence the performance of the approach. For example, a facial recognition algorithm may perform poorly when image resolution is low or images are taken in low lighting. Or a speech-to-text system might not be used reliably to provide closed captions for online lectures because it fails to handle technical jargon.
- The authors should discuss the computational efficiency of the proposed algorithms and how they scale with dataset size.
- If applicable, the authors should discuss possible limitations of their approach to address problems of privacy and fairness.
- While the authors might fear that complete honesty about limitations might be used by reviewers as grounds for rejection, a worse outcome might be that reviewers discover limitations that aren't acknowledged in the paper. The authors should use their best judgment and recognize that individual actions in favor of transparency play an important role in developing norms that preserve the integrity of the community. Reviewers will be specifically instructed to not penalize honesty concerning limitations.

# 3. Theory assumptions and proofs

Question: For each theoretical result, does the paper provide the full set of assumptions and a complete (and correct) proof?

Answer: [NA] Guidelines:

- The answer NA means that the paper does not include theoretical results.
- All the theorems, formulas, and proofs in the paper should be numbered and cross-referenced.
- All assumptions should be clearly stated or referenced in the statement of any theorems.
- The proofs can either appear in the main paper or the supplemental material, but if they appear in the supplemental material, the authors are encouraged to provide a short proof sketch to provide intuition.
- Inversely, any informal proof provided in the core of the paper should be complemented by formal proofs provided in appendix or supplemental material.
- Theorems and Lemmas that the proof relies upon should be properly referenced.

#### 4. Experimental result reproducibility

Question: Does the paper fully disclose all the information needed to reproduce the main experimental results of the paper to the extent that it affects the main claims and/or conclusions of the paper (regardless of whether the code and data are provided or not)?

Answer: [Yes]

Justification: The paper provides sufficient details regarding the model architecture, training settings, data preprocessing, and evaluation metrics, enabling reproduction of the main experimental results and verification of the core claims.

#### Guidelines:

- The answer NA means that the paper does not include experiments.
- If the paper includes experiments, a No answer to this question will not be perceived well by the reviewers: Making the paper reproducible is important, regardless of whether the code and data are provided or not.
- If the contribution is a dataset and/or model, the authors should describe the steps taken to make their results reproducible or verifiable.
- Depending on the contribution, reproducibility can be accomplished in various ways. For example, if the contribution is a novel architecture, describing the architecture fully might suffice, or if the contribution is a specific model and empirical evaluation, it may be necessary to either make it possible for others to replicate the model with the same dataset, or provide access to the model. In general, releasing code and data is often one good way to accomplish this, but reproducibility can also be provided via detailed instructions for how to replicate the results, access to a hosted model (e.g., in the case of a large language model), releasing of a model checkpoint, or other means that are appropriate to the research performed.
- While NeurIPS does not require releasing code, the conference does require all submissions to provide some reasonable avenue for reproducibility, which may depend on the nature of the contribution. For example
- (a) If the contribution is primarily a new algorithm, the paper should make it clear how to reproduce that algorithm.
- (b) If the contribution is primarily a new model architecture, the paper should describe the architecture clearly and fully.
- (c) If the contribution is a new model (e.g., a large language model), then there should either be a way to access this model for reproducing the results or a way to reproduce the model (e.g., with an open-source dataset or instructions for how to construct the dataset).
- (d) We recognize that reproducibility may be tricky in some cases, in which case authors are welcome to describe the particular way they provide for reproducibility. In the case of closed-source models, it may be that access to the model is limited in some way (e.g., to registered users), but it should be possible for other researchers to have some path to reproducing or verifying the results.

#### 5. Open access to data and code

Question: Does the paper provide open access to the data and code, with sufficient instructions to faithfully reproduce the main experimental results, as described in supplemental material?

Answer: [Yes]

Justification: The source code is included in the supplementary materials to facilitate reproducibility and further research.

#### Guidelines:

- The answer NA means that paper does not include experiments requiring code.
- Please see the NeurIPS code and data submission guidelines (https://nips.cc/public/guides/CodeSubmissionPolicy) for more details.
- While we encourage the release of code and data, we understand that this might not be possible, so "No" is an acceptable answer. Papers cannot be rejected simply for not including code, unless this is central to the contribution (e.g., for a new open-source benchmark).
- The instructions should contain the exact command and environment needed to run to reproduce the results. See the NeurIPS code and data submission guidelines (https://nips.cc/public/guides/CodeSubmissionPolicy) for more details.
- The authors should provide instructions on data access and preparation, including how to access the raw data, preprocessed data, intermediate data, and generated data, etc.
- The authors should provide scripts to reproduce all experimental results for the new proposed method and baselines. If only a subset of experiments are reproducible, they should state which ones are omitted from the script and why.
- At submission time, to preserve anonymity, the authors should release anonymized versions (if applicable).
- Providing as much information as possible in supplemental material (appended to the paper) is recommended, but including URLs to data and code is permitted.

#### 6. Experimental setting/details

Question: Does the paper specify all the training and test details (e.g., data splits, hyperparameters, how they were chosen, type of optimizer, etc.) necessary to understand the results?

Answer: [Yes]

Justification: Training and testing details are described in Appendix A. The hyperparameter search ranges and sensitivity analysis are provided in Appendix J.

#### Guidelines:

- The answer NA means that the paper does not include experiments.
- The experimental setting should be presented in the core of the paper to a level of detail that is necessary to appreciate the results and make sense of them.
- The full details can be provided either with the code, in appendix, or as supplemental material.

# 7. Experiment statistical significance

Question: Does the paper report error bars suitably and correctly defined or other appropriate information about the statistical significance of the experiments?

Answer: [NA] Guidelines:

- The answer NA means that the paper does not include experiments.
- The authors should answer "Yes" if the results are accompanied by error bars, confidence intervals, or statistical significance tests, at least for the experiments that support the main claims of the paper.
- The factors of variability that the error bars are capturing should be clearly stated (for example, train/test split, initialization, random drawing of some parameter, or overall run with given experimental conditions).

- The method for calculating the error bars should be explained (closed form formula, call to a library function, bootstrap, etc.)
- The assumptions made should be given (e.g., Normally distributed errors).
- It should be clear whether the error bar is the standard deviation or the standard error
  of the mean.
- It is OK to report 1-sigma error bars, but one should state it. The authors should preferably report a 2-sigma error bar than state that they have a 96% CI, if the hypothesis of Normality of errors is not verified.
- For asymmetric distributions, the authors should be careful not to show in tables or figures symmetric error bars that would yield results that are out of range (e.g. negative error rates).
- If error bars are reported in tables or plots, The authors should explain in the text how they were calculated and reference the corresponding figures or tables in the text.

# 8. Experiments compute resources

Question: For each experiment, does the paper provide sufficient information on the computer resources (type of compute workers, memory, time of execution) needed to reproduce the experiments?

Answer: [Yes]

Justification: The paper provides sufficient details on the computational resources used, including the type of GPU, memory, and training time, in Section 4.1. This information allows readers to estimate the resources required for reproduction.

#### Guidelines:

- The answer NA means that the paper does not include experiments.
- The paper should indicate the type of compute workers CPU or GPU, internal cluster, or cloud provider, including relevant memory and storage.
- The paper should provide the amount of compute required for each of the individual experimental runs as well as estimate the total compute.
- The paper should disclose whether the full research project required more compute than the experiments reported in the paper (e.g., preliminary or failed experiments that didn't make it into the paper).

#### 9. Code of ethics

Question: Does the research conducted in the paper conform, in every respect, with the NeurIPS Code of Ethics https://neurips.cc/public/EthicsGuidelines?

Answer: [Yes]

Justification: We have read the NeurIPS Code of Ethics, and we are certain that the paper conform to it.

#### Guidelines:

- The answer NA means that the authors have not reviewed the NeurIPS Code of Ethics.
- If the authors answer No, they should explain the special circumstances that require a deviation from the Code of Ethics.
- The authors should make sure to preserve anonymity (e.g., if there is a special consideration due to laws or regulations in their jurisdiction).

# 10. Broader impacts

Question: Does the paper discuss both potential positive societal impacts and negative societal impacts of the work performed?

Answer: [Yes]

Justification: The paper discusses both potential positive and negative societal impacts of the proposed method in Appendix M.

# Guidelines:

• The answer NA means that there is no societal impact of the work performed.

- If the authors answer NA or No, they should explain why their work has no societal impact or why the paper does not address societal impact.
- Examples of negative societal impacts include potential malicious or unintended uses (e.g., disinformation, generating fake profiles, surveillance), fairness considerations (e.g., deployment of technologies that could make decisions that unfairly impact specific groups), privacy considerations, and security considerations.
- The conference expects that many papers will be foundational research and not tied to particular applications, let alone deployments. However, if there is a direct path to any negative applications, the authors should point it out. For example, it is legitimate to point out that an improvement in the quality of generative models could be used to generate deepfakes for disinformation. On the other hand, it is not needed to point out that a generic algorithm for optimizing neural networks could enable people to train models that generate Deepfakes faster.
- The authors should consider possible harms that could arise when the technology is being used as intended and functioning correctly, harms that could arise when the technology is being used as intended but gives incorrect results, and harms following from (intentional or unintentional) misuse of the technology.
- If there are negative societal impacts, the authors could also discuss possible mitigation strategies (e.g., gated release of models, providing defenses in addition to attacks, mechanisms for monitoring misuse, mechanisms to monitor how a system learns from feedback over time, improving the efficiency and accessibility of ML).

# 11. Safeguards

Question: Does the paper describe safeguards that have been put in place for responsible release of data or models that have a high risk for misuse (e.g., pretrained language models, image generators, or scraped datasets)?

Answer: [NA] Guidelines:

- The answer NA means that the paper poses no such risks.
- Released models that have a high risk for misuse or dual-use should be released with
  necessary safeguards to allow for controlled use of the model, for example by requiring
  that users adhere to usage guidelines or restrictions to access the model or implementing
  safety filters.
- Datasets that have been scraped from the Internet could pose safety risks. The authors should describe how they avoided releasing unsafe images.
- We recognize that providing effective safeguards is challenging, and many papers do
  not require this, but we encourage authors to take this into account and make a best
  faith effort.

#### 12. Licenses for existing assets

Question: Are the creators or original owners of assets (e.g., code, data, models), used in the paper, properly credited and are the license and terms of use explicitly mentioned and properly respected?

Answer: [Yes]

Justification: All external assets used in the paper, including datasets and code, are properly credited. Their licenses and terms of use are explicitly acknowledged and respected.

#### Guidelines:

- The answer NA means that the paper does not use existing assets.
- The authors should cite the original paper that produced the code package or dataset.
- The authors should state which version of the asset is used and, if possible, include a URL.
- The name of the license (e.g., CC-BY 4.0) should be included for each asset.
- For scraped data from a particular source (e.g., website), the copyright and terms of service of that source should be provided.

- If assets are released, the license, copyright information, and terms of use in the
  package should be provided. For popular datasets, paperswithcode.com/datasets
  has curated licenses for some datasets. Their licensing guide can help determine the
  license of a dataset.
- For existing datasets that are re-packaged, both the original license and the license of the derived asset (if it has changed) should be provided.
- If this information is not available online, the authors are encouraged to reach out to the asset's creators.

#### 13. New assets

Question: Are new assets introduced in the paper well documented and is the documentation provided alongside the assets?

Answer: [Yes]

Justification: The new assets introduced in this paper, including the implementation code and model components, are well documented. Documentation is provided alongside the code in the supplementary materials.

#### Guidelines:

- The answer NA means that the paper does not release new assets.
- Researchers should communicate the details of the dataset/code/model as part of their submissions via structured templates. This includes details about training, license, limitations, etc.
- The paper should discuss whether and how consent was obtained from people whose asset is used.
- At submission time, remember to anonymize your assets (if applicable). You can either create an anonymized URL or include an anonymized zip file.

# 14. Crowdsourcing and research with human subjects

Question: For crowdsourcing experiments and research with human subjects, does the paper include the full text of instructions given to participants and screenshots, if applicable, as well as details about compensation (if any)?

Answer: [NA]

#### Guidelines:

- The answer NA means that the paper does not involve crowdsourcing nor research with human subjects.
- Including this information in the supplemental material is fine, but if the main contribution of the paper involves human subjects, then as much detail as possible should be included in the main paper.
- According to the NeurIPS Code of Ethics, workers involved in data collection, curation, or other labor should be paid at least the minimum wage in the country of the data collector.

# 15. Institutional review board (IRB) approvals or equivalent for research with human subjects

Question: Does the paper describe potential risks incurred by study participants, whether such risks were disclosed to the subjects, and whether Institutional Review Board (IRB) approvals (or an equivalent approval/review based on the requirements of your country or institution) were obtained?

Answer: [NA]

# Guidelines:

- The answer NA means that the paper does not involve crowdsourcing nor research with human subjects.
- Depending on the country in which research is conducted, IRB approval (or equivalent) may be required for any human subjects research. If you obtained IRB approval, you should clearly state this in the paper.

- We recognize that the procedures for this may vary significantly between institutions and locations, and we expect authors to adhere to the NeurIPS Code of Ethics and the guidelines for their institution.
- For initial submissions, do not include any information that would break anonymity (if applicable), such as the institution conducting the review.

# 16. Declaration of LLM usage

Question: Does the paper describe the usage of LLMs if it is an important, original, or non-standard component of the core methods in this research? Note that if the LLM is used only for writing, editing, or formatting purposes and does not impact the core methodology, scientific rigorousness, or originality of the research, declaration is not required.

Answer: [NA] Guidelines:

- The answer NA means that the core method development in this research does not involve LLMs as any important, original, or non-standard components.
- Please refer to our LLM policy (https://neurips.cc/Conferences/2025/LLM) for what should or should not be described.

#### A Dataset

We evaluate the performance of TFPS on eight widely used datasets, including four ETT datasets (ETTh1, ETTh2, ETTm1 and ETTm2), Exchange, Weather, Electricity, and ILI. This subsection provides a summary of the datasets:

- ETT<sup>2</sup> [70] (Electricity Transformer Temperature) dataset contains two electric transformers, ETT1 and ETT2, collected from two separate counties. Each of them has two versions of sampling resolutions (15min & 1h). Thus, there are four ETT datasets: ETTm1, ETTm2, ETTh1, and ETTh2.
- Exchange-Rate <sup>3</sup> [23] the exchange-rate dataset contains the daily exchange rates of eight foreign countries including Australia, British, Canada, Switzerland, China, Japan, New Zealand, and Singapore ranging from 1990 to 2016.
- Weather <sup>4</sup> [62] dataset contains 21 meteorological indicators in Germany, such as humidity and air temperature.
- Electricity <sup>5</sup> [62] is a dataset that describes 321 customers' hourly electricity consumption.
- **Traffic** <sup>6</sup> [62] is a dataset featuring hourly road occupancy rates from 862 sensors along the freeways in the San Francisco Bay area.
- ILI <sup>7</sup> [62] dataset collects the number of patients and influenza-like illness ratio in a weekly frequency.

For the data split, we follow [69] and split the data into training, validation, and testing by a ratio of 6:2:2 for the ETT datasets and 7:1:2 for the others. Details are shown in Table 5. The best parameters are selected based on the lowest validation loss and then applied to the test set for performance evaluation. The data and codes are available: https://github.com/syrGitHub/TFPS.

Table 5: The statistics of the datasets.

	The state of the s													
Datasets	Variates	Prediction Length	Timesteps	Granularity	Average Wasserstein * (Time Domain)	Average Wasserstein* (Frequency Domain)								
ETTh1	7	{96, 192, 336, 720}	17,420	1 hour	9.268	11.561								
ETTh2	7	{96, 192, 336, 720}	17,420	1 hour	13.221	18.970								
ETTm1	7	{96, 192, 336, 720}	69,680	15 min	9.336	10.660								
ETTm2	7	{96, 192, 336, 720}	69,680	15 min	13.606	16.574								
Exchange-Rate	8	{96, 192, 336, 720}	7,588	1 day	0.132	0.144								
Weather	21	{96, 192, 336, 720}	52,696	10 min	39.742	77.422								
Electricity	321	{96, 192, 336, 720}	26,304	1 hour	520.162	1018.311								
Traffic	862	{96, 192, 336, 720}	17,451	1 hour	0.011	0.028								
ILI	7	{24, 36, 48, 60}	966	1 week	258881.714	381377.494								

<sup>\*</sup> A large Wasserstein indicates a more severe drift.

# **B** Related Work

Deep learning has achieved remarkable success across diverse domains such as computer vision [14, 38, 39, 40, 37], natural language processing [58, 6], and multi-modality [13, 15], and has also advanced the state of the art in time series modeling [56, 19].

The Combination of Time and Frequency Domains. Time-domain models excel at capturing sequential trends, while frequency-domain models are essential for identifying periodic and oscillatory patterns. Recent research has increasingly emphasized integrating information from both domains to better interpret underlying patterns. For instance, ATFN [66] demonstrates the advantage of frequency domain methods for forecasting strongly periodic time series through a time–frequency adaptive

<sup>&</sup>lt;sup>2</sup>https://github.com/zhouhaoyi/ETDataset

<sup>3</sup>https://github.com/laiguokun/multivariate-time-series-data

<sup>4</sup>https://www.bgc-jena.mpg.de/wetter/

<sup>&</sup>lt;sup>5</sup>https://archive.ics.uci.edu/ml/datasets/ElectricityLoadDiagrams20112014

<sup>6</sup>http://pems.dot.ca.gov

<sup>&</sup>lt;sup>7</sup>https://gis.cdc.gov/grasp/fluview/fluportaldashboard.html

network. TFDNet [42] adopts a branching structure to capture long-term latent patterns and temporal periodicity from both domains. Similarly, JTFT [4] utilizes the frequency domain representation to extract multi-scale dependencies while enhancing local relationships modeling through time domain representation. TFMRN [65] expands data in both domains to capture finer details that may not be evident in the original data. Recently, TSLANet [9] leverages Fourier analysis to enhance feature representation and capture both long-term and short-term interactions.

Building on these approaches, our proposed method, TFPS, introduces a novel Dual-Domain Encoder that effectively combines time and frequency domain information to capture both trend and periodic patterns. By integrating time-frequency features, TFPS significantly advances the field in addressing the complexities inherent in time series forecasting.

**Mixture-of-Experts.** Mixture-of-Experts (MoE) models have gained attention for their ability to scale efficiently by activating only a subset of experts for each input, as first introduced by [57]. Despite their success, challenges such as training instability, expert redundancy, and limited expert specialization have been identified [50, 5]. These issues hinder the full potential of MoE models in real-world tasks.

Recent advances have integrated MoE with Transformers to improve scalability and efficiency. For example, GLaM [7] and Switch Transformer [12] interleave MoE layers with Transformer blocks, reducing computational costs. Other models like state space models (SSMs) [49, 2], [1] combines MoE with alternative architectures for enhanced scalability and inference speed.

In contrast, our approach introduces MoE into time series forecasting by assigning experts to specific time-frequency patterns, enabling more effective, patch-level adaptation. This approach represents a significant innovation in time series forecasting, offering a more targeted and effective way to handle varying patterns across both time and frequency domains.

# C Wasserstein Distance

The Wasserstein distance, also called the Earth mover's distance or the optimal transport distance, is a similarity metric between two probability distributions. In the discrete case, the Wasserstein distance can be understood as the cost of an optimal transport plan to convert one distribution into the other. The cost is calculated as the product of the amount of probability mass being moved and the distance it is being moved.

Given two one-dimensional probability mass functions, u and v, the first Wasserstein distance between them is defined as:

$$l_1(u,v) = \inf_{\pi \in \Gamma(u,v)} \int_{\mathbb{R} \times \mathbb{R}} |x - y| \, d\pi(x,y), \tag{13}$$

where  $\Gamma(u,v)$  is the set of (probability) distributions on  $\mathbb{R} \times \mathbb{R}$  whose marginals are u and v on the first and second factors respectively. Here, u(x) represents the probability of u at position x, with the same interpretation for v(x).

In the special case of one-dimensional distributions, the Wasserstein distance can be equivalently expressed using their cumulative distribution functions (CDFs), U and V, as:

$$l_1(u,v) = \int_{-\infty}^{+\infty} |U - V|. \tag{14}$$

This equivalence is rigorously proved in [54].

The input distributions can be empirical, therefore coming from samples whose values are effectively inputs of the function, or they can be seen as generalized functions, in which case they are weighted sums of Dirac delta functions located at the specified values.

# **D** Distribution Shifts in both Time and Frequency Domains

The time series  $\mathcal{X}$  is segmented into N patches, where each patch  $\mathcal{P}_n = \{x_{n1}, x_{n2}, \dots, x_{nP}\}$  consists of P consecutive timesteps for  $n = 1, 2, \dots, N$ . For the frequency domain, we apply a Fourier transform  $\mathcal{F}$  to each patch  $\mathcal{P}_n$ , obtaining its frequency-domain representation as  $\hat{\mathcal{P}}_n = \mathcal{F}(\mathcal{P}_n)$ .

Each patch's probability distribution in the time domain is denoted as  $p_t(\mathcal{P}_n)$ , representing the statistical properties of  $\mathcal{P}_n$ , while its frequency domain distribution, denoted as  $p_f(\hat{\mathcal{P}}_n)$ , captures its spectral characteristics.

The distribution shifts between two patches  $\mathcal{P}_i$  and  $\mathcal{P}_j$  are characterized by the comparing their probability distributions in both time and frequency domains. These shifts are defined as:

$$\mathcal{D}_t(\mathcal{P}_i, \mathcal{P}_j) = |d(p_t(\mathcal{P}_i), p_t(\mathcal{P}_j))| > \theta, \tag{15}$$

$$\mathcal{D}_f(\hat{\mathcal{P}}_i, \hat{\mathcal{P}}_i) = |d(p_f(\hat{\mathcal{P}}_i), p_f(\hat{\mathcal{P}}_i))| > \theta, \tag{16}$$

where d is a distance metric, such as Wasserstein distance or Kullback-Leibler divergence, and  $\theta$  is a threshold indicating a significant distribution shift. If  $\mathcal{D}_t(\mathcal{P}_i, \mathcal{P}_j)$  or  $\mathcal{D}_f(\hat{\mathcal{P}}_i, \hat{\mathcal{P}}_j)$  exceeds  $\theta$ , this implies a significant distribution shift between the two patches in either domain. It is important to note that  $\theta$  serves only as a conceptual threshold for defining distribution shifts in the analysis and does not participate in the modeling or training process of TFPS.

#### **E** Metric Illustration

We use mean square error (MSE) and mean absolute error (MAE) as our metrics for evaluation of all forecasting models. Then calculation of MSE and MAE can be described as:

$$MSE = \frac{1}{H} \sum_{i=L+1}^{L+H} (\hat{Y}_i - Y_i)^2,$$
 (17)

$$MAE = \frac{1}{H} \sum_{i=L+1}^{L+H} |\hat{Y}_i - Y_i|,$$
 (18)

where  $\hat{Y}$  is predicted vector with H future values, while Y is the ground truth.

In addition, we report the IMP (Improvement) metric, which is defined as:

$$IMP = \frac{Avg MSE \text{ of baselines} - MSE \text{ of TFPS}}{Avg MSE \text{ of baselines}} \times 100\%.$$
 (19)

This metric quantifies the relative percentage improvement of TFPS over the average MSE of all baseline methods. A higher IMP value indicates better overall performance of TFPS compared to the baselines.

#### F Hyperparameter-search Results

# F.1 Comparsion with Specific Models

To ensure a fair comparison between models, we conducted experiments using unified parameters and reported results in the main text.

In addition, considering that the reported results in different papers are mostly obtained through hyperparameter search, we provide the experiment results with the full version of the parameter search. We searched for input length among 96, 192, 336, and 512. The results are included in Table 6. All baselines are reproduced by their official code.

We can find that the relative promotion of TFPS over TFDNet is smaller under comprehensive hyperparameter search than the unified hyperparameter setting. It is worth noticing that TFPS runs much faster than TFDNet according to the efficiency comparison in Table 12. Therefore, considering performance, hyperparameter-search cost and efficiency, we believe TFPS is a practical model in real-world applications and is valuable to deep time series forecasting community.

# F.2 Comparsion with Foundation Models

Table 7 presents the detailed results of TFPS compared to recent foundation models (AutoTimes [30], Moment [16], and Timer [32]) across six datasets and four forecasting lengths. Consistent

Table 6: Experiment results under hyperparameter searching for the long-term forecasting task. The best results are highlighted in **bold** and the second best are underlined.

M	odel	IMP.	TF (O		TSL.	ANet (24)	FI (20	TS (24)	iTrans	former	TFDN (20	Net-IK	Patcl (20	nTST (23)		esNet (23)	Dlii (20			ormer (22)
M	etric	MSE	MSE	MAE	MSE	MAE	MSE	MAE	MSE	MAE	MSE	MAE	MSE	MAE	MSE	MAE	MSE	MAE	MSE	MAE
ETTh1	96 192 336 720	1.5% 5.7% 9.8% 11.2%	0.372 0.401 0.409 0.423	0.404 0.410 0.402 0.433	0.368 0.413 <u>0.412</u> 0.473	$\begin{array}{c} \underline{0.394} \\ 0.418 \\ \underline{0.416} \\ 0.477 \end{array}$	0.374 0.407 0.429 <u>0.425</u>	0.395 0.414 0.428 <u>0.446</u>	0.387 0.441 0.491 0.509	0.405 0.436 0.463 0.494	0.360 0.403 0.434 0.437	0.387 0.412 0.429 0.452	0.375 0.414 0.432 0.450	0.400 0.421 0.436 0.466	0.389 0.441 0.491 0.512	0.412 0.442 0.467 0.491	0.384 0.443 0.447 0.504	0.405 0.450 0.448 0.515	0.385 0.441 0.491 0.501	0.425 0.461 0.473 0.499
ETTh2	96 192 336 720	9.3% 10.4% 17.7% 9.0%	0.268 0.329 0.329 0.412	0.325 0.376 0.401 0.441	0.283 0.331 <b>0.319</b> 0.407	0.344 0.378 0.377 0.449	0.274 0.337 0.360 0.386	0.337 0.377 0.398 0.423	0.301 0.380 0.424 0.430	0.350 0.399 0.432 0.447	0.271 0.333 0.361 0.382	0.329 0.372 0.396 0.418	0.278 0.339 0.336 <b>0.382</b>	0.336 0.380 0.380 0.421	0.324 0.393 0.429 0.433	0.368 0.410 0.437 0.448	0.290 0.388 0.463 0.733	0.353 0.422 0.473 0.606	0.342 0.434 0.512 0.467	0.383 0.440 0.497 0.476
ETTm1	96 192 336 720	8.5% 8.2% 8.2%	0.281 0.324 0.359 0.409	0.329 0.354 0.404 0.408	0.291 0.329 <b>0.357</b> 0.423	0.353 0.372 0.392 0.425	0.303 0.337 0.372 0.428	0.345 0.365 <u>0.385</u> 0.416	0.342 0.383 0.418 0.487	0.377 0.396 0.418 0.457	$\begin{array}{c} \underline{0.283} \\ \underline{0.327} \\ 0.361 \\ \underline{0.411} \end{array}$	0.330 0.356 <b>0.375</b> 0.409	0.288 0.334 0.367 0.417	0.342 0.372 0.393 0.422	0.337 0.395 0.433 0.484	0.377 0.406 0.432 0.458	0.301 0.336 0.372 0.427	0.345 0.366 0.389 0.423	0.360 0.395 0.448 0.491	0.406 0.427 0.458 0.479
ETTm2	96 192 336 720	8.9% 5.7% 8.5% 12.0%	0.158 0.222 0.268 0.344	0.243 0.302 0.316 0.373	0.167 0.221 0.277 0.356	0.256 0.294 0.329 0.382	0.165 0.220 0.274 0.367	0.255 0.291 0.326 0.383	0.186 0.254 0.316 0.414	0.272 0.314 0.351 0.407	0.158 0.219 0.273 0.346	0.244 0.282 0.317 0.374	0.164 0.221 0.277 0.365	0.253 0.292 0.329 0.384	0.182 0.252 0.312 0.417	0.262 0.307 0.346 0.404	0.172 0.237 0.295 0.427	0.267 0.314 0.359 0.439	0.193 0.256 0.321 0.434	0.285 0.324 0.364 0.426
Traffic	96 192 336 720	17.8% 17.0% 17.2% 15.7%	0.370 0.390 0.401 0.432	0.250 0.258 0.271 0.294	0.375 0.395 0.402 0.431	0.260 0.272 0.272 <b>0.288</b>	0.398 0.408 0.420 0.448	0.285 0.288 0.292 0.310	0.428 0.448 0.465 0.501	0.295 0.302 0.311 0.333	0.377 0.391 0.408 0.451	0.253 0.260 <b>0.266</b> 0.291	0.373 0.395 0.402 0.435	0.259 0.273 0.274 0.293	0.586 0.618 0.634 0.659	0.316 0.323 0.337 0.349	0.413 0.424 0.438 0.466	0.287 0.290 0.299 0.316	0.575 0.613 0.622 0.630	0.357 0.381 0.380 0.383
Electricity	96 192 336 720	10.3% 11.9% 6.8% 6.9%	0.128 0.145 0.166 0.198	0.220 0.235 0.258 0.283	0.137 0.153 0.165 0.206	0.229 0.242 0.263 0.294	0.135 0.149 0.165 0.204	0.231 0.244 0.260 0.293	0.148 0.167 0.178 0.211	0.239 0.258 0.271 0.300	0.130 0.146 0.162 0.201	0.222 0.237 <b>0.254</b> 0.287	0.130 0.149 0.168 0.204	0.223 0.240 0.262 0.289	0.168 0.186 0.196 0.235	0.272 0.289 0.297 0.329	0.140 0.154 0.169 0.204	0.237 0.250 0.268 0.300	0.188 0.197 0.212 0.243	0.303 0.311 0.327 0.352
	1st Co	ount	3	2	:	5	(	0	(	)	1	0		1	(	0	(	)	(	)

Table 7: Detailed results of the comparison between TFPS and foundation models. The best results are highlighted in **bold** and the second best are underlined.

Model		IMP.		PS ur)		Times (24)		ment (24)		ner (24)
Metric	;	MSE	MSE	MAE	MSE	MAE	MSE	MAE	MSE	MAE
	96	-2.2%	0.372	0.404	0.365	0.405	0.369	0.406	0.359	0.392
ETTh1	192	-1.3%	0.401	0.410	0.392	0.423	0.405	0.431	0.391	0.413
EIIII	336	0.5%	0.409	0.402	0.406	0.433	0.420	0.441	0.407	0.424
	720	3.1%	0.423	0.433	0.423	0.450	0.466	0.479	0.421	0.441
	96	6.3%	0.268	0.325	0.286	0.349	0.287	0.347	0.285	0.344
ETTh2	192	9.2%	0.329	0.376	0.351	0.393	0.371	0.401	0.365	0.400
EIInz	336	17.2%	0.329	0.401	0.377	0.417	0.404	0.425	0.412	0.440
	720	9.8%	0.412	0.441	0.439	0.464	0.463	0.476	0.467	0.487
	96	1.3%	0.281	0.329	0.297	0.350	0.281	0.343	0.276	0.335
ETTm1	192	1.2%	0.324	0.354	0.344	0.377	0.318	0.368	0.323	0.365
Ellmi	336	1.6%	0.359	0.404	0.380	0.398	0.356	0.391	0.358	0.388
	720	4.8%	0.409	0.408	0.433	0.431	0.438	0.441	0.419	0.423
	96	8.6%	0.158	0.243	0.181	0.266	0.170	0.258	0.167	0.254
ETTm2	192	5.5%	0.222	0.302	0.241	0.306	0.233	0.301	0.229	0.297
ETTIIIZ	336	6.9%	0.268	0.316	0.295	0.341	0.287	0.340	0.282	0.335
	720	8.1%	0.344	0.373	0.376	0.393	0.371	0.399	0.376	0.398
	96	-5.5%	0.370	0.250	0.347	0.249	0.360	0.254	0.345	0.237
Traffic	192	-5.3%	0.390	0.258	0.366	0.258	0.381	0.265	0.365	0.247
Hanne	336	-3.1%	0.401	0.271	0.383	0.267	0.404	0.277	0.381	0.256
	720	-1.1%	0.432	0.294	0.420	0.286	0.438	0.297	0.424	0.280
	96	3.4%	0.128	0.220	0.135	0.230	0.133	0.236	0.130	0.224
Electricity	192	4.3%	0.145	0.235	0.153	0.247	0.152	0.254	0.149	0.243
Electricity	336	1.5%	0.166	0.258	0.172	0.266	0.166	0.265	0.168	0.263
	720	5.2%	0.198	0.283	0.212	0.300	0.202	0.298	0.213	0.303
1 <sup>st</sup>	1st Count			0	2	2		2	1	4

with Table 6, for TFPS, we searched input lengths among 96, 192, 336, and 512, and report the best-performing configuration for each forecasting length.

TFPS achieves the best performance in **30 out of 48** settings, significantly outperforming AutoTimes and Moment, which only achieve 2 best scores each. Although Timer demonstrates competitive

Table 8: Detailed results of the comparison between TFPS and normalization-based methods using FEDformer. The best results are highlighted in **bold** and the second best are underlined.

								FEDf	ormer			
M	odel	IMP.	TF	PS	+ 5	SIN	+ S	AN	+ Dis	sh-TS	+ Re	evIN
			(O	ur)	(20	24)	(20	23)	(20	23)	(20	21)
M	etric	MSE	MSE	MAE								
_	96	-0.9%	0.398	0.413	0.413	0.372	0.383	0.409	0.390	0.424	0.392	0.413
ETTh1	192	3.7%	0.423	0.423	0.443	0.417	0.431	0.438	0.441	0.458	0.443	0.444
덢	336	-0.5%	0.484	0.461	0.465	0.448	0.471	0.456	0.495	0.486	0.495	0.467
	720	4.8%	0.488	0.476	0.509	0.490	0.504	0.488	0.519	0.509	0.520	0.498
	96	34.0%	0.313	0.355	0.412	0.357	0.300	0.355	0.806	0.589	0.380	0.402
ETTh2	192	28.3%	0.405	0.410	0.472	0.453	0.392	0.413	0.936	0.659	0.457	0.443
덢	336	38.2%	0.392	0.415	0.527	0.527	0.459	0.462	1.039	0.702	0.515	0.479
	720	41.4%	0.410	0.433	0.593	0.639	0.462	0.472	1.237	0.759	0.507	0.487
_	96	4.5%	0.327	0.367	0.373	0.320	0.311	0.355	0.348	0.397	0.340	0.385
ETTm1	192	2.9%	0.374	0.395	0.394	0.366	0.351	0.383	0.406	0.428	0.390	0.411
덢	336	4.4%	0.401	0.408	0.418	0.405	0.390	0.407	0.438	0.450	0.432	0.436
	720	-0.8%	0.479	0.456	0.451	0.475	0.456	0.444	0.497	0.481	0.497	0.466
7	96	37.5%	0.170	0.255	0.326	0.211	0.175	0.266	0.394	0.395	0.192	0.272
ETTm2	192	35.9%	0.235	0.296	0.402	0.316	0.246	0.315	0.552	0.472	0.270	0.320
E	336	38.6%	0.297	0.335	0.465	0.399	0.315	0.362	0.808	0.601	0.348	0.367
	720	40.2%	0.401	0.397	0.555	0.547	0.412	0.422	1.282	0.771	0.430	0.415
is	96	30.7%	0.154	0.202	0.280	0.215	0.179	0.239	0.244	0.317	0.187	0.234
Weather	192	25.6%	0.205	0.249	0.314	0.264	0.234	0.296	0.320	0.380	0.235	0.272
Νe	336	22.0%	0.262	0.289	0.329	0.293	0.304	0.348	0.424	0.452	0.287	0.307
	720	21.3%	0.344	0.342	0.382	0.370	0.400	0.404	0.604	0.553	0.361	0.353
	1st Co	ount	2	4	Ģ	)		7	(	)	(	)

Table 9: Detailed results of the comparison between TFPS and normalization-based methods using DLinear. The best results are highlighted in **bold** and the second best are <u>underlined</u>.

			T)	TDC.				DLi	near			
Mode	el	IMP.	TF	PS	+ 5	SIN	+ S	AN	+ Dis	sh-TS	+ R	evIN
			(O	ur)	(20	24)	(20	23)	(20	23)	(20	21)
Metri	c	MSE	MSE	MAE	MSE	MAE	MSE	MAE	MSE	MAE	MSE	MAE
	96	-1.6%	0.398	0.413	0.401	0.415	0.385	0.395	0.389	0.399	0.393	0.416
	192	2.9%	0.423	0.423	0.438	0.456	0.432	0.423	0.443	0.433	0.431	0.428
ETTh1	336	-0.4%	0.484	0.461	0.458	0.436	0.490	0.463	0.443	0.456	0.488	0.423
	720	4.6%	$\frac{0.484}{0.488}$	0.476	0.515	0.500	0.490	0.504	0.523	0.508	0.493	0.482
									<u>'</u>			
	96	4.9%	0.313	0.355	0.359	0.359	0.319	0.364	0.317	0.365	0.322	0.361
ETTh2	192	1.1%	0.405	0.410	0.409	0.424	0.407	0.439	0.408	0.420	0.412	0.424
BITHE	336	3.6%	0.392	0.415	0.398	0.429	0.411	0.425	0.416	0.426	0.403	0.427
	720	2.7%	0.410	0.433	0.419	0.442	0.417	0.441	0.428	0.439	0.422	0.446
	96	4.9%	0.327	0.367	0.350	0.383	0.333	0.374	0.343	0.375	0.352	0.369
ETTm1	192	1.9%	0.374	0.395	0.383	0.396	0.374	0.396	0.381	0.391	0.388	0.396
EIImi	336	3.0%	0.401	0.408	0.413	0.416	0.406	0.418	0.416	0.417	0.419	0.414
	720	0.0%	0.479	0.456	0.473	0.452	0.483	0.451	0.482	0.458	0.478	0.463
	96	5.5%	0.170	0.255	0.172	0.283	0.179	0.272	0.189	0.264	0.179	0.269
ETTm2	192	4.4%	0.235	0.296	0.249	0.301	0.239	0.316	0.249	0.302	0.248	0.302
EIIIIIZ	336	1.2%	0.297	0.335	0.299	0.339	0.301	0.353	0.305	0.349	0.299	0.345
	720	3.2%	0.401	0.397	0.412	0.421	0.404	0.408	0.429	0.402	0.411	0.402
	96	4.5%	0.154	0.202	0.162	0.223	0.157	0.215	0.173	0.241	0.154	0.243
Waathan	192	7.6%	0.205	0.249	0.216	0.259	0.214	0.258	0.225	0.263	0.233	0.265
Weather	336	6.8%	0.262	0.289	0.279	0.291	0.275	0.292	0.289	0.305	0.282	0.293
	720	3.0%	0.344	0.342	0.355	0.341	0.349	0.351	0.366	0.369	0.348	0.362
1 <sup>st</sup>	Coun	t	3	3	1	3		3		1	(	)

performance (with 14 best scores), TFPS consistently achieves lower error in datasets with higher distribution shifts, such as ETTh2 and ETTm2, indicating its advantage in handling pattern heterogeneity.

These results reinforce the effectiveness of TFPS's pattern-specific modeling strategy, especially in scenarios where traditional large-scale foundation models struggle to generalize.

Table 10: Comparison between TFPS and MoE-based methods. The best results are highlighted in **bold** and the second best are <u>underlined</u>.

Mode	el	IMP.		PS ur)		LE (24)		oU (24)		4TSF 24)
Metr	ic	MSE	MSE	MAE	MSE	MAE	MSE	MAE	MSE	MAE
	96	-4.3%	0.398	0.413	0.383	0.392	0.381	0.403	0.382	0.400
ETTh1	192	1.7%	0.423	0.423	0.434	0.426	0.429	0.430	0.430	0.426
EIIII	336	1.6%	0.484	0.461	0.489	0.478	0.488	0.463	0.498	0.467
	720	8.2%	0.488	0.476	0.602	0.545	0.499	0.484	0.494	0.479
	96	10.4%	0.313	0.355	0.413	0.360	0.317	0.358	0.318	0.358
ETTh2	192	10.3%	0.405	0.410	0.525	0.416	0.409	0.414	0.419	0.414
E11n2	336	7.1%	0.392	0.415	0.423	0.434	0.397	0.420	0.447	0.452
	720	8.4%	0.410	0.433	0.453	0.458	0.412	0.434	0.477	0.476
	96	13.5%	0.327	0.367	0.338	0.380	0.465	0.442	0.333	0.371
ETTm1	192	10.6%	0.374	0.395	0.388	0.403	0.483	0.455	0.384	0.399
EIIIII	336	11.8%	0.401	0.408	0.417	0.431	0.540	0.488	0.407	0.413
	720	7.3%	0.479	0.456	0.486	0.472	0.583	0.509	0.483	0.469
	96	13.9%	0.170	0.255	0.238	0.271	0.179	0.263	0.175	0.260
ETTm2	192	3.8%	0.235	0.296	0.247	0.305	0.243	0.303	0.244	0.305
L1 IIIIZ	336	3.3%	0.297	0.335	0.308	0.343	0.306	0.343	0.308	0.347
	720	13.7%	0.401	0.397	0.583	0.419	0.405	0.404	0.405	0.404
1s	1st Count		3	0		1		1	(	)

# **G** Compared with Other Methods

#### **G.1** Compared with Normalization Methods

In this section, we provide the detailed experimental results of the comparison between TFPS and five state-of-the-art normalization methods for non-stationary time series forecasting: SIN [17], SAN [34], Dish-TS [10], and RevIN [20]. We summarize the forecasting results of TFPS and baseline models in Table 8 and Table 9. Specifically, the results of FEDformer combined with SIN are taken from [17], while those of FEDformer with other normalization-based methods are reported by [34]. For a fair comparison, we additionally rerun all experiments for DLinear combined with each normalization method.

Table 8 and Table 9 presents the forecasting performance across all prediction lengths for each dataset, along with the relative improvements of TFPS over existing methods. As shown, TFPS consistently achieves the best performance in the majority of settings, demonstrating its strong adaptability to distributional and conceptual drifts in time series data.

We attribute this improvement to the accurate identification of pattern groups and the provision of specialized experts for each group, thereby avoiding the over-stationarization problem often associated with normalization methods.

# G.2 Compared with MoE-based Methods

As shown in Table 10, unlike MoE-based methods that rely on the Softmax function as a gating mechanism, our approach constructs a pattern recognizer to assign different experts to handle distinct patterns. This results in TFPS achieving relative improvements of 2.3%, 9.0%, 10.6%, and 9.1% across the four datasets, respectively.

#### **G.3** Compared with Distribution Shift Methods

As shown in Table 11, we compare with the methods for distribution shift. This results in TFPS achieving relative improvements of 6.7%, 6.6%, 4.8%, and 5.9% across the four datasets, respectively.

# **H** Model Analysis

**Detailed Results on the Number of Experts.** We provide the full results on the number of experts for the ETTh1 and Weather dataset in Figure 7.

Table 11: Comparison between TFPS and methods for Distribution Shift. The best results are highlighted in **bold** and the second best are <u>underlined</u>.

Mode	el	IMP.	l	PS ur)		opa 24))		LID (24)	l	Net 24)
Metr	ic	MSE	MSE	MAE	MSE	MAE	MSE	MAE	MSE	MAE
	96	7.9%	0.398	0.413	0.385	0.407	0.440	0.439	0.425	0.402
ETTh1	192	10.3%	0.423	0.423	0.445	0.434	0.492	0.466	0.452	0.443
EIIII	336	4.9%	0.484	0.461	0.489	0.460	0.525	0.481	0.492	0.482
	720	4.4%	0.488	0.476	0.497	0.480	0.517	0.496	0.504	0.496
	96	10.6%	0.313	0.355	0.318	0.360	0.318	0.359	0.382	0.362
ETTh2	192	4.7%	0.405	0.410	0.378	0.398	0.414	0.418	0.435	0.426
EIIIIZ	336	4.8%	0.392	0.415	0.415	0.430	0.398	0.421	0.426	0.419
	720	6.8%	0.410	0.433	0.445	0.456	0.424	0.441	0.456	0.437
	96	6.8%	0.327	0.367	0.329	0.359	0.329	0.370	0.374	0.392
ETTm1	192	2.0%	0.374	0.395	0.380	0.393	0.379	0.400	0.385	0.435
LIIIII	336	8.7%	0.401	0.408	0.401	0.411	0.405	0.412	0.473	0.458
	720	2.0%	0.479	0.456	0.475	0.448	0.482	0.464	0.496	0.483
	96	5.3%	0.170	0.255	0.179	0.261	0.175	0.258	0.184	0.274
ETTm2	192	3.8%	0.235	0.296	0.246	0.305	0.241	0.302	0.248	0.384
LI IIIIZ	336	3.4%	0.297	0.335	0.310	0.348	0.303	0.342	0.313	0.374
	720	9.0%	0.401	0.397	0.405	0.402	0.456	0.436	0.425	0.438
1s	1st Count		2	5	(	5	(	)		1

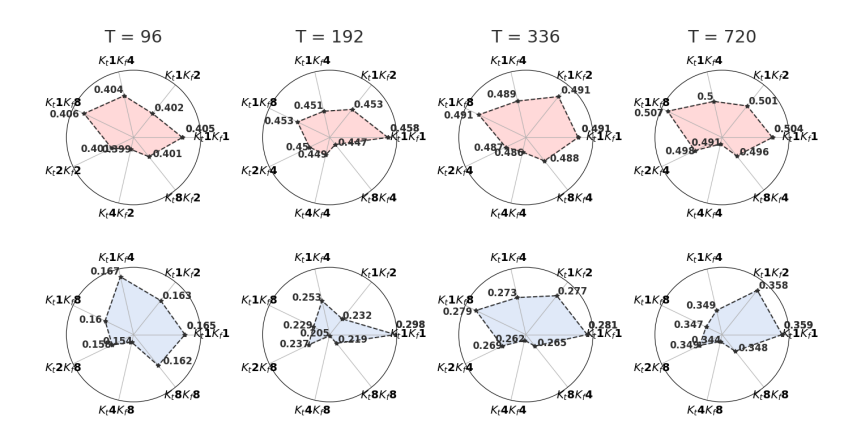


Figure 7: Results of expert number experiments for ETTh1 and Weather.

In Figure 7, we set the learning rate to 0.0001 and conducted four sets of experiments on the ETTh1 and Weather datasets,  $K_t = 1$ ,  $K_f = \{1, 2, 4, 8\}$ , to explore the effect of the number of frequency experts on the results. For example,  $K_t 1 K_f 4$  means that the TFPS contains 1 time experts and 4 frequency experts. We observed that  $K_t 1 K_f 2$  outperformed  $K_t 1 K_f 4$  in most cases, suggesting that increasing the number of experts does not always lead to better performance.

In addition, we conducted three experiments based on the optimal number of frequency experts to verify the impact of varying the number of time experts on the results. As shown in Figure 7, the best results for ETTh1 were obtained with  $K_t 4K_f 2$ ,  $K_t 8K_f 4$ ,  $K_t 4K_f 4$ ,  $K_t 4K_f 4$ , while for Weather, the optimal results were achieved with  $K_t 4K_f 8$ ,  $K_t 4K_f 8$ ,  $K_t 4K_f 4$  and  $K_t 4K_f 8$ . Combined with the average Wasserstein in Table 5, we attribute this to the fact that, in cases where concept drift is more severe, such as Weather, more experts are needed, whereas fewer experts are sufficient when the drift is less severe.

Comparing Inter- and Intra-Cluster Differences via Wasserstein Distance. To assess the effectiveness of the PI module, we replace it with a linear layer and compare the resulting inter- and intra-cluster Wasserstein distance heatmaps in Figure 8. The diagonal elements represent the average Wasserstein distances of patches within the same clusters. If these values are small, it indicates that the difference of patches within the same cluster is relatively similar. The off-diagonal elements represent

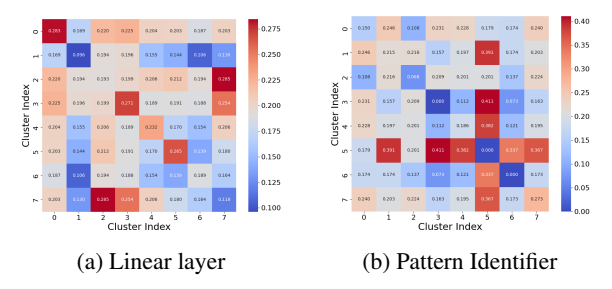


Figure 8: Heatmap showing the Wasserstein distances of inter- and intra-cluster patches on ETTh1.

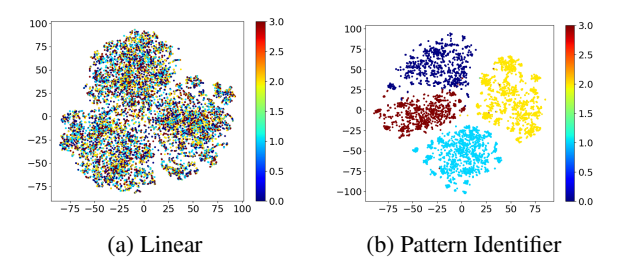


Figure 9: Visualization of the embedded representations with t-SNE on ETTh1 for the time domain with H=96. (a) t-SNE visualization with a Linear Layer replacing the Patch Identifier for comparison. (b) t-SNE visualization of TFPS.

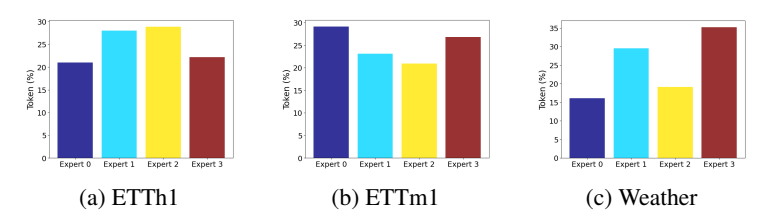


Figure 10: MoE Expert allocation distributions of TFPS: the x-axis corresponds to the 4 experts, and the y-axis shows the proportion of tokens assigned to each expert.

the average Wasserstein distances between patches from different clusters, where larger values mean significant differences between the clusters. We observe that when using PI, the intra-cluster drift is smaller, while the inter-cluster shift is more pronounced compared to the linear layer. This indicates that our identifier effectively classifies and distinguishes between different patterns.

TFPS produces differentiated token embeddings by adapting to the characteristics of the data. Figure 9 presents the t-SNE visualization of the learned embedded representation on the ETTh1 for the time domain with H=96. In the Figure 9 (a), where the pattern identifier is replaced with a linear layer, the representation lacks clear clustering structures, resulting in scattered and indistinct groupings. In contrast, Figure 9 (b) shows the visualization of the representation learned by the proposed method, which effectively captures discriminative features and reveals significantly clearer clustering patterns.

**TFPS** implements dataset-specific token embeddings assignment in a data-driven way, effectively improving performance. Figure 10 visualizes the expert allocation distributions across various datasets. Notably, ETTh1 and ETTm1 exhibit a high degree of consistency in their expert assignments, underscoring the model's ability to capture shared patterns. Conversely, the Weather dataset shows a distinctly different allocation pattern, highlighting the method's sensitivity to unique dataset characteristics and its capability to tailor expert assignments accordingly.

Table 12: The GPU memory (MB) and speed (inference time) of each model.

	TFPS	TSLANet	FITS	iTransformer	TFDNet-IK	PatchTST	TimesNet	DLinear	FEDformer
MSE	0.423	0.448	0.445	0.441	0.458	0.460	0.441	0.434	0.441
GPU Memory (MB)	9.643	0.481	0.019	3.304	0.246	0.205	2.345	0.142	62.191
Average Inference Time (ms)	6.114	0.063	1.184	2.571	98.266	4.861	12.306	0.659	136.130

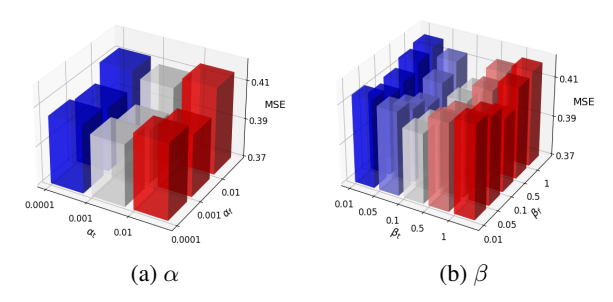


Figure 11: Parameter sensitivity of  $\alpha$  and  $\beta$  of the proposed method on the ETTh1-96 dataset.

# I Efficiency Analysis

To make this clearer, we present the results of ETTh1 for a prediction length of 192 from Table 1 and include additional results on runtime and computational complexity in Table 12. Due to the sparsity of MoPE, TFPS achieves a balance between performance and efficiency:

**Performance Superiority**. TFPS achieves an MSE of 0.423, outperforming TSLANet (0.448), FITS (0.445), PatchTST (0.460), and FEDformer (0.441). This represents a 5.6% improvement over TSLANet and a 8.0% improvement over PatchTST, highlighting its significant accuracy gains. While DLinear achieves an MSE of 0.434, TFPS still demonstrates a 2.5% relative improvement, making it the most accurate model among all baselines.

Efficiency Gains. TFPS maintains competitive runtime and memory efficiency.

- Runtime: TFPS runs in 6.457 ms, making it  $2.8 \times$  faster than PatchTST (17.851 ms) and  $11.2 \times$  faster than TimesNet (72.196 ms).
- Memory Usage: TFPS uses 9.643 MB of GPU memory, significantly less than FEDformer (62.191 MB) and comparable to iTransformer (3.304 MB). This makes TFPS suitable for resource-constrained applications while maintaining superior performance.

**Balancing Trade-offs**. While lightweight models like DLinear (0.434 MSE, 0.789 ms runtime) are slightly more efficient, TFPS delivers a performance improvement of 2.5%, providing a well-rounded solution that balances accuracy and efficiency effectively.

# J Hyperparameter Sensitivity

In this section, we analysis the impact of the hyperparameters  $\alpha$  and  $\beta$  on the performance.

Specifically, we performed a grid search to optimize the hyperparameters  $\alpha_t = \{0.0001, 0.001, 0.001, 0.01\}$  and  $\alpha_f = \{0.0001, 0.001, 0.01\}$ , as shown in Figure 11 (a). After extensive testing, we ultimately fixed at  $\alpha_t = \alpha_f = 10^{-3}$  in our experiments.

In addition, we conducted a grid search to optimize the balance factors  $\beta_t = \{0.01, 0.05, 0.1, 0.5, 1\}$  and  $\beta_f = \{0.01, 0.05, 0.1, 0.5, 1\}$ . The performance under different parameter values is displayed in Figure 11 (b), from which we have the following observations:

- Firstly, the performance is affected when the value of  $\beta$  is too low, indicating that the proposed clustering objective plays a crucial role in distinguishing patterns.
- Second, an excessive  $\beta$  also has a negative on the performance. One plausible explanation is that the excessive value influences the learning of the inherent structure of original data, resulting in a perturbation of the embedding space.

Table 13: In the table, w/ Imaginary indicates that we incorporate both the real and imaginary parts into the network.

		ET'	Th1		ETTh2				
	96	192	336	720	96	192	336	720	
TFPS w/ Imaginary	0.398	0.423	0.484	0.488	0.313	0.405	0.392	0.410	
w/ Imaginary	0.397	0.424	0.487	0.486	0.312	0.406	0.391	0.	

Table 14: Ablation study of PI components. The model variants in our ablation study include the following configurations across both time and frequency branches: (a) inclusion of the Time PI; (b) inclusion of the Frequency PI; (c) exclusion of both. The best results are in **bold**.

Time PI	Frequency PI	ETTh1				ETTh2			
		96	192	336	720	96	192	336	720
✓	✓	0.398	0.423	0.484	0.488	0.313	0.405	0.392	0.410
<b>√</b>	Х	0.404	0.454	0.490	0.503	0.322	0.413	0.410	0.425
X	$\checkmark$		0.456						
X	×	0.407	0.458	0.497	0.513	0.328	0.418	0.419	0.435

• Overall, we recommend setting  $\beta$  around 0.1 for optimal performance.

#### **K** Full Ablation

#### K.1 Impacts of Real/Imaginary Parts

To further validate the robustness of our approach, we adopted similar operations in FreTS to conduct experiments incorporating both the real and imaginary parts. The results in the Table 13 show that the performance of TFPS with the real part only is very similar to that when both parts are included, while requiring fewer parameters. This further reinforces the conclusion that TFPS remains highly effective even when focusing solely on the real part of the Fourier transform.

# K.2 Ablation on PI

The PI module plays a crucial role in identifying and characterizing distinct patterns within the time series data, while the gating network dynamically selects the most relevant experts for each segment. This collaborative mechanism allows the model to specialize in handling different patterns and adapt effectively to distribution shifts, thus mitigating the overfitting risks that arise from treating all data equally.

To validate the importance of PI empirically, we have conducted the ablation experiments comparing the model's performance by replacing the PI module with a linear layer in the Table 2 of main text. In addition, we supplement some ablation experiments in Table 14 to further verify the effectiveness of PI.

# **K.3** Ablation on $R_1$ and $R_2$

We conducted ablation experiments to further verify the important roles of  $R_1$  and  $R_2$ , as shown in Table 15.

#### **K.4** Replace MoPE with Alternative Designs

Here we provide the complete results of alternative designs for TFPS.

As show in Table 16, we have conducted addition experiments where we replaced the MoPE module with weighted multi-output predictor and stacked self-attention layers, keeping all other components

Table 15: Ablation study of Loss Constraint. The model variants in our ablation study include the following configurations across both time and frequency branches: (a) inclusion of the  $R_1$ ; (b) inclusion of the  $R_2$ ; (c) exclusion of both. The best results are in **bold**.

$R_1$ $R_2$	$R_0$		ET	Γh1	ETTh2					
	96	192	336	720	96	192	336	720		
<b>√</b>	✓	0.398	0.423	0.484	0.488	0.313	0.405	0.392	0.410	
<b>√</b>	Х	0.408	0.449	0.500	0.498	0.320	0.418	0.415	0.429	
X	$\checkmark$	$\frac{0.403}{0.412}$	0.434	0.493	0.491	0.316	0.413	0.405	<u>0.418</u>	
X	X	0.412	0.456	0.509	0.503	0.328	0.425	0.420	0.435	

Table 16: Multi-output predictor and a stacked attention layer are used to replace MoPE in ETTh1 and ETTh2 datasets.

	ETTh1				ETTh2			
	96	192	336	720	96	192	336	720
TFPS	0.398	0.423	0.484	0.488	0.313	0.405	0.392	0.410
Multi-output Predictor	0.403	0.435	0.492	0.491	0.317	0.407	0.399	0.425
Attention Layers	0.399	0.452	0.492	0.508	0.334	0.407	0.409	0.451

and configurations identical. The results demonstrate that our proposed method significantly outperforms them, which validates the importance of the Top-K selection and pattern-aware design in enhancing the model's representation capacity. In contrast, multi-output predictor and self-attention typically treats all data points uniformly, which may limit its ability to capture subtle distribution shifts or evolving patterns across patches.

# L Algorithm of TFPS

We provide the pseudo-code of TFPS in Algorithm 1.

# M Broader Impact

**Real-world Applications.** TFPS addresses the crucial challenge of time series forecasting, which is a valuable and urgent demand in extensive applications. Our method achieves consistent state-of-the-art performance in four real-world applications: electricity, weather, exchange rate, illness. Researchers in these fields stand to benefit significantly from the enhanced forecasting capabilities of TFPS. We believe that improved time series forecasting holds the potential to empower decision-making and proactively manage risks in a wide array of societal domains.

**Academic Research.** TFPS draws inspiration from classical time series analysis and stochastic process theory, contributing to the field by introducing a novel framework with the assistance pattern recognition. This innovative architecture and its associated methodologies represent significant advancements in the field of time series forecasting, enhancing the model's ability to address distribution shifts and complex patterns effectively.

**Model Robustness.** Extensive experimentation with TFPS reveals robust performance without exceptional failure cases. Notably, TFPS exhibits impressive results and maintains robustness in datasets with distribution shifts. The pattern identifier structure within TFPS groups the time series into distinct patterns and adopts a mixture of pattern experts for further prediction, thereby alleviating prediction difficulties. However, it is essential to note that, like any model, TFPS may face challenges when dealing with unpredictable patterns, where predictability is inherently limited. Understanding these nuances is crucial for appropriately applying and interpreting TFPS's outcomes.

Our work only focuses on the scientific problem, so there is no potential ethical risk.

```
Algorithm 1 Time-Frequency Pattern-Specific architecture - Overall Architecture.
```

**Input**: Input lookback time series  $X \in \mathbb{R}^{L \times C}$ ; input length L; predicted length H; variables number C; patch length P; feature dimension D; encoder layers number n; random Gaussian distribution-initialized subspace  $\mathbf{D} = [\mathbf{D}^{(1)}, \mathbf{D}^{(2)}, \cdots, \mathbf{D}^{(K)}]$ , each  $\mathbf{D}^{(j)} \in \mathbf{R}^{q \times d}$ , where  $q = C \times D$  and d = q/K. Technically, we set D as 512, n as 2.

**Output**: The prediction result  $\hat{Y}$ .

```
\triangleright X \in \mathbb{R}^{C \times L} \triangleright X_t^0 \in \mathbb{R}^{C \times N \times D}
  1: X = X.transpose
  2: X_{PE} = \text{Patch}(X) + \text{Position Embedding}
  3: ▷ Time Encoder.
  4: X_t^0 = X_{PE}
  5: for l in \{1, \ldots, n\}:
            X_t^{l-1} = \text{LayerNorm} (X_t^{l-1} + \text{Self-Attn}(X_t^{l-1})).

X_t^{l} = \text{LayerNorm} (X_t^{l-1} + \text{Feed-Forward}(X_t^{l-1})).
                                                                                                                                         \triangleright X_t^{l-1} \in \mathbb{R}^{C \times N \times D}\triangleright X_t^l \in \mathbb{R}^{C \times N \times D}
  8: End for
                                                                                                                                                  \triangleright z_t^l \in \mathbb{R}^{C \times N \times D}
  9: z_t = X_t^l
 10: ⊳ Pattern Identifier for Time Domain.

ho Eq. 6 of the paper s_t \in \mathbb{R}^{C \times N \times D}
11: s_t = \text{Subspace affinity}(z_t, \mathbf{D})
                                                                                                                  \triangleright Eq. 7 of the paper \hat{s}_t \in \mathbb{R}^{C \times N \times D}
12: \hat{s}_t = \texttt{Subspace refinement}(s_t)
13: ▷ Mixture of Temporal Pattern Experts.
14: G(s) = \text{Softmax} (\text{TopK}(s_t))
15: h_t = \sum_{k=1}^K G(s) \text{MLP}_k(z_t)
                                                                                         \triangleright Eq. 10 and Eq. 11 of the paper h_t \in \mathbb{R}^{C \times N \times D}
 16: ⊳ Frequency Encoder.
17: X_f^0 = X_{PE}
                                                                                                              \triangleright Eq. 2 of the paper X_f^0 \in \mathbb{R}^{C \times N \times P}
18: for l in \{1, \ldots, n\}:

19: X_f^{l-1} = \text{LayerNorm}(X_f^{l-1} + \text{Fourier}(X_f^{l-1})).

20: X_f^l = \text{LayerNorm}(X_f^{l-1} + \text{Feed-Forward}(X_f^{l-1})).
                                                                                                                                          \triangleright X_f^{l-1} \in \mathbb{R}^{C \times N \times D}\triangleright X_f^{l} \in \mathbb{R}^{C \times N \times D}
21: End for
                                                                                                                                                 \triangleright z_f^n \in \mathbb{R}^{C \times N \times D}
22: z_f = X_f^l
23: ▶ Pattern Identifier for Frequency Domain.
                                                                                                                \triangleright Eq. 6 of the paper s_f \in \mathbb{R}^{C \times N \times D}
24: s_f = \text{Subspace affinity}(z_f, \mathbf{D})
                                                                                                                 \triangleright Eq. 7 of the paper \hat{s}_f \in \mathbb{R}^{C \times N \times D}
25: \hat{s}_f = \text{Subspace refinement}(s_f)
26: ▷ Mixture of Frequency Pattern Experts.
27: G(s) = \text{Softmax} (\text{TopK}(s_f))
28: h_f = \sum_{k=1}^{K} G(s) MLP_k(z_f)
                                                                                         \triangleright Eq. 10 and Eq. 11 of the paper h_f \in \mathbb{R}^{C \times N \times D}
                                                                                                                                                \triangleright h \in \mathbb{R}^{C \times N \times 2*D}
29: h = \operatorname{Concat}(h_t, h_f)
30: for c in \{1, \ldots, C\}:
                                                                                  \triangleright Project tokens back to predicted series \hat{Y} \in \mathbb{R}^{C \times H}
             \hat{Y} = \text{Linear (Flatten } (h)).
32: End for
33: \hat{Y} = \hat{Y}.\texttt{transpose}
                                                                                                                                                         \triangleright \hat{Y} \in \mathbb{R}^{H \times C}
                                                                                                         \triangleright Output the final prediction \hat{Y} \in \mathbb{R}^{H \times C}
34: Return \hat{Y}
```

# **N** Limitations

Though TFPS demonstrates promising performance on the benchmark dataset, there are still some limitations of this method. First, the patch length is primarily chosen heuristically, and the current design struggles with handling indivisible lengths or multi-period characteristics in time series. While this approach works well in experiments, it lacks generalizability for real-world applications. Second, the real-world time series data undergo expansion, implying that the new patterns continually emerge over time, such as an epidemic or outbreak that had not occurred before. Therefore, future work will focus on developing a more flexible and automatic patch length selection mechanism, as well as an extensible solution to address these evolving distribution shifts.